

POLITECNICO DI TORINO

Corso di Laurea Magistrale in Ingegneria Energetica e Nucleare

Tesi di Laurea Magistrale

“System-level modeling of the storage unit and auxiliary components of a line-focusing concentrating solar collector-based power plant”



Relatori:

Prof. Zanino Roberto

Ing. Cagnoli Mattia

Candidato:

Tomatis Davide

25 marzo 2021

Contents

0. Abstract.....	6
1. Introduction.....	7
2. Thesis structure	8
2.1. Aim of the Thesis.....	8
2.2 Contents of the thesis.....	8
3. The concentrated solar power	9
3.1 The history.....	9
3.2 The strengths of CSP	10
3.3 The downsides of CSP	11
4. The components.....	12
4.1 The typical configurations of CSP plants.....	12
4.2 The collectors	12
4.2.1 Solar dishes.....	12
4.2.2 Solar towers.....	13
4.2.3 Parabolic trough.....	14
4.2.4 Linear Fresnel Collectors.....	15
4.3 The heat transfer fluids	16
4.4 The storage systems	17
4.4.1 The sensible heat storage	17
4.4.2 The latent heat storage	18
4.5 The backup systems.....	18
5. The reference plant.....	19
5.1 The plant.....	19
5.2 The two-tank storage	20
5.3 The pumping stations.....	20
5.4 The solar field.....	21
6. The system-level model	21
6.1 The storage	21
6.1.1 The molten salt stored	21
6.1.2 The air layer	23
6.1.3 The walls.....	23
6.1.4 The system-tank.....	24
6.1.5 A tank performance verification.....	25
6.2 The backup heater	26
6.3 The pumping system	26
6.4 The power block.....	27
6.5 The solar block.....	27

7.	The simulations.....	28
7.1	The framework.....	28
7.2	The regulated pump performance.....	29
7.3	The complete system simulation.....	32
7.4	The morning startup simulation.....	33
8.	Conclusions.....	35
9.	Perspectives.....	35
10.	Bibliography.....	36

0. Abstract

The Concentrating Solar Power (CSP) technology converts the energy of the concentrated sun light in thermal energy at middle-high temperature, which can be stored in a thermal energy storage (TES) unit or directly used to drive a convectional thermodynamic cycle (power unit). The CSP systems are a promising solution for the generation of dispatchable renewable electricity because of the TES that allows decoupling the electricity generation from the intermittent solar source. However, CSP plants can also produce other assets, mainly hydrogen or fresh water, or they can make use of fossil fuels to increase its flexibility: this plant modification is called hybridization.

The most diffuse concentration technology among CSP plants is the parabolic trough (PT) system. It adopts long strings of parabolic mirrors to focus the solar radiation onto a linear receiver, typically an encapsulated and evacuated tube, which transfers the energy of the concentrated sun light to a heat transfer fluid (HTF). An alternative line-focusing system is the Fresnel technology that uses a set of almost flat mirrors strips instead of the parabolic concentrator. The state of the art of the TES technology for line-focusing systems is the two-tank sensible heat thermal storage that uses molten salts as storage medium.

The aim of this thesis consists of the development of a thermal-fluid-dynamic system-level model of a CSP plant based on the line-focusing technology using the Modelica (object-oriented) language. This thesis was performed in collaboration with the FATA E.P.C. Company, located in Italy (Torino), which kindly provided data about the line-focusing CSP plant of Partanna (Sicily).

The model should include the solar field of mirrors, the receiver unit, the TES (two-tank configuration), the pumping stations and the gas-fired unit that provides additional flexibility to the system, while the modeling of the power unit is out of the scope of the work. Molten salts are used both as HTF and as storage medium. The solar field and the receiver model have been already developed at Politecnico, while the rest of system-level model is developed in the framework of this thesis. The final system-level model is capable of providing the thermal performance (i.e., the heat lost towards the environment) of the single components and of the plant as a whole, in a steady state and under various operational conditions.

1. Introduction

Today the world electricity grids are crossing a revolution period, as a consequence of the rising fractions of renewable energy among the providers. In particular, a growth amounting to more than 25% of the solar energy sector is driving the shift from a centralized, non-renewable and large-scale production to a decentralized, low-carbon and spatially distributed electricity generation. [1]

However, photovoltaic (PV), wind and a part of hydroelectric power production are affected by the intermittent nature of the source that makes difficult providing dispatchable electricity. Hence, even if currently renewable sources are the best solutions for decarbonization, of the global economy together with carbon capture and storage and a reduction of consumption, it is necessary to couple them to a series of technologies capable of preventing blackouts and continuously satisfy the demand. [2]

In the last ten years, the biggest nations replaced part of the coal and petrol consumption, which have a high carbon footprint, with natural gas, exploiting the technological improvements about combined cycle plants and open cycle turbines, which result in lower CO₂ emissions. This is the USA case, which since 2008 has halved the electricity produced with coal and almost tripled the natural gas consumption. [3] But this solution cannot be definitive, as renewable sources can: in addition to unavoidable carbon emissions as a consequence of combustion, the entire supply chain is exposed to non-negligible methane (Global Warming Potential = 25) losses, which are estimated in the USA in a range between 2% and 19%, depending on the assumptions about measurement process. [4]

Solar power is essential in the future, since the sun is the primary source of almost all the energy for the world (except for geothermal energy); the potential for solar energy is extremely large, because it is estimated at about 200.000 times the world overall daily electric generation, but the difficulty lies in converting it into a dispatchable form. [5] But also PV energy has a non-negligible carbon footprint compared to other renewable sources (connected to the panel realization and decommissioning) and it is directly produced as electricity, so it is not easy to store in large scale. However, as forecasts are still characterized by an error and the energy availability is not constant, it can represent a problem for the grid safety. [6] For instance, during May 2019, in California, a series of curtailments were forced to a fraction of the rooftop panels to avoid congestion to the grid [7] [8]: such events have involved a financial loss and demonstrated how it is not trivial the power management where variable renewable energies (VRE) are prevailing.

In the framework where European Union's long-term strategy consists of reaching carbon neutrality within 2050 [9], China has announced to have set the same target for 2060 [10] and other states aim to do it in the future like Canada [11], it is necessary to introduce with sources that can be used on demand to ensure the electric stability and net zero emissions. Since the pumped-hydro plants have a strong environmental impact and its market in the richest nations looks to be almost saturated, currently one of the best solutions for an effective energy storage looks to be the concentrated solar power. [12]

Concentrated solar power uses the concentration of solar energy on a receiver crossed by a heat transfer fluid, HTF, to increase its temperature until a value sufficiently high to feed a thermodynamic cycle (typically a Rankine loop, but also Stirling). Concentration is possible through four technologies and the plants are usually coupled to other energy sources used as a backup. The key advantage of CSP, which makes this solution more attractive than PV, is the opportunity to store a large quantity of thermal energy, which allows decoupling the harvesting of the solar energy from the electricity production. This asset is named TES, thermal energy storage.

For what concerns the fight against the global warming, CSP and PV have the almost same the same impact (about $60 \div 70 \text{ g}_{CO_2}/kWh_{el}$), which is not as brilliant as for wind power ($20 \div 50 \text{ g}_{CO_2}/kWh_e$), but it is still one order of magnitude smaller than in the case of coal. [6] [13] The reason for this is mainly due to the massive request for heat transfer fluid, the mirrors and structural material, which makes the plant realization impactful.

2. Thesis structure

2.1. Aim of the Thesis

This Master Thesis aims to focus on the strength of CSP technologies, the storage system, to allocate it into a real plant and test its performance in realistic cases. A thermal-fluid-dynamic system-level model of the plant has been produced by using the Modelica (object-oriented) language to carry out simulations. This work was performed in collaboration with the FATA E.P.C. Company, located in Italy (Torino), which gently supplied measurements and data about the line-focusing CSP plant of Partanna (Sicily, Italy).

The approach used in this thesis exploits the upside of Modelica language, namely the possibility to split the components into several sub-models. The system-level model includes the solar field of concentrators (linear Fresnel reflectors), the receiver unit, the TES (two-tank configuration), the pumping stations and the backup system (gas-fired unit), while the power unit is out of the scope of the work. The HTF and the storage medium are the same, namely molten salts. The solar field and the receiver model have been already developed at Politecnico, while the remaining part of system-level model is built in the context of this thesis.

The complete system-level model is developed to simulate the plant in each component, providing the thermal performance in a steady state and under various operational conditions.

2.2 Contents of the thesis

In this thesis an analysis of the concentrated solar power evolution is proposed, to show its perspectives and the projects oriented to a massive development of the technology. Then, an engineering description of the devices composing the plants is performed, with positive and negative aspects of each solution.

The presentation of the elements of the system is then followed by the description of the physics, the chosen correlations and the assumptions at the base of the models, with a view of their integration in the plant. The framework in which it is expected to work is realistic, hence a brief description of the boundary conditions and a justification for their selection are proposed.

At the end, the results of simulations about the single components and the whole plant are shown, succeeded by conclusions drawn and possible perspectives.

3. The concentrated solar power

3.1 The history

The first episode in which humanity concentrated solar rays to generate heat is mysterious, but the legend goes that Archimedes had the idea to defend Greek coasts of Sicily against roman navy by using a “burning glass”. [14] Probably this is simply a legend, and historians do not agree about the real feasibility, but it tells that people in the past already knew this concept. Besides, before being able to manage and directly use such heat, no one has never been interested in exploiting it.

The first person who translated the burning glass concept into a useful form was Auguste Mouchout: he produced steam by using an ancestral parabolic trough system in 1866, when the internal combustion engine was rising in the technological landscape. [15] Many other prototypes followed this in the following century, but the first real plant working and generating 1 MW superheated steam at 500°C was that commissioned by Professor Giovanni Francia in 1968 in Genoa. Thirteen years later, in California, the first tower plant named “Solar One” was set in operation with a nominal output of 10 MW; this paved the way to a decade of exponential growth, reaching a total production of 300 MW in 1990. [15]

Such a growth stopped until 2007, when in Australia, in the United States and in Spain, a series of companies exploited the technological improvements in the CSP field provided by the research. Thus, as a consequence of the completion of new plants started at the beginning of the decade, the rise of the power output emerged again, even if braked by the economic crisis; this has been possible thanks to a rising environmental care and need for not variable renewable sources. At the end of 2019, the world concentrated solar power production amounts to around 6.5 GW. [16]

In the Figure 1 and Figure 2 it is possible to observe the different behavior of the curves after 2014, the technological enhancements have increased the average performance in terms of equivalent hours, obtaining a higher production from the same installed size.

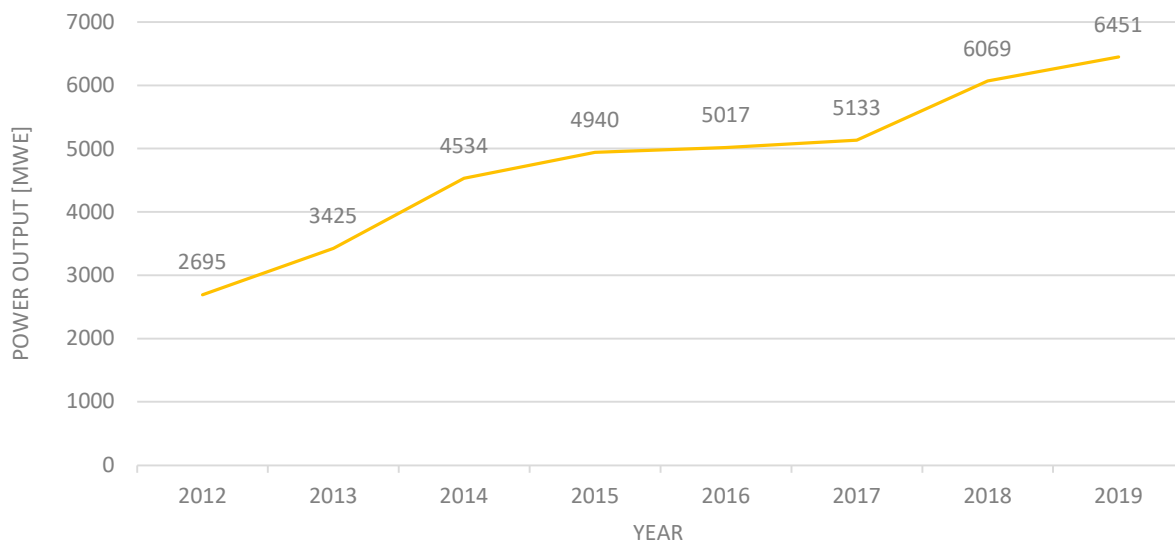


Figure 1 - The evolution of the world CSP electric power output [16]

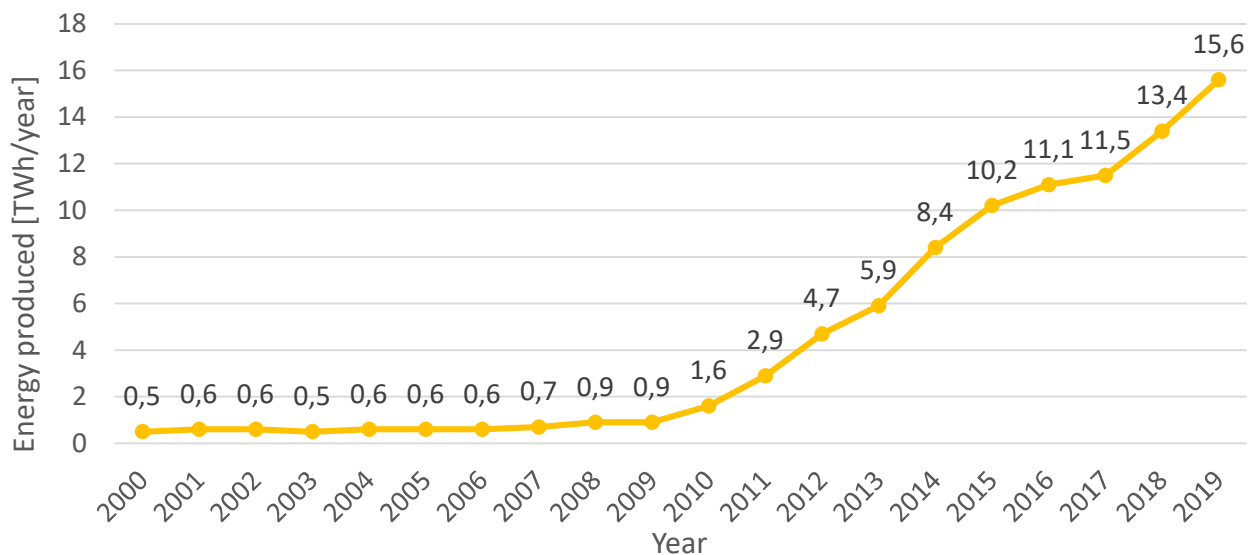


Figure 2 – Yearly electricity production by CSP plants in the world [35]

3.2 The strengths of CSP

As mentioned before, concentrated solar is the only renewable energy source which can be regulated together with pumped hydro, but it is less impactful on the territory because located in hot regions. In particular, to obtain a sufficiently high solar irradiance, it is necessary to build the plant in a dry region, located close to the Tropics but possibly far from the sea. The reason lies in the fact that atmospheric moisture works as a filter for light and where trade winds are predominant, air is typically extremely dry and stable. Moreover, the more the location is set in the vicinity of the Equator, the smaller is the oscillation of the duration of the day during the year.

As it is visible in the Figure 3, the regions where the global horizontal irradiation is higher are located exactly in dry and tropical areas, like the Sahara Desert, Southern US, Brazil, Chile, Southern China, Australia and other deserts. Indeed, this part of the Planisphere is named Sun Belt. Also altitude can give a contribution, due to a thinner atmospheric air layer (it should be noted Atacama Desert).

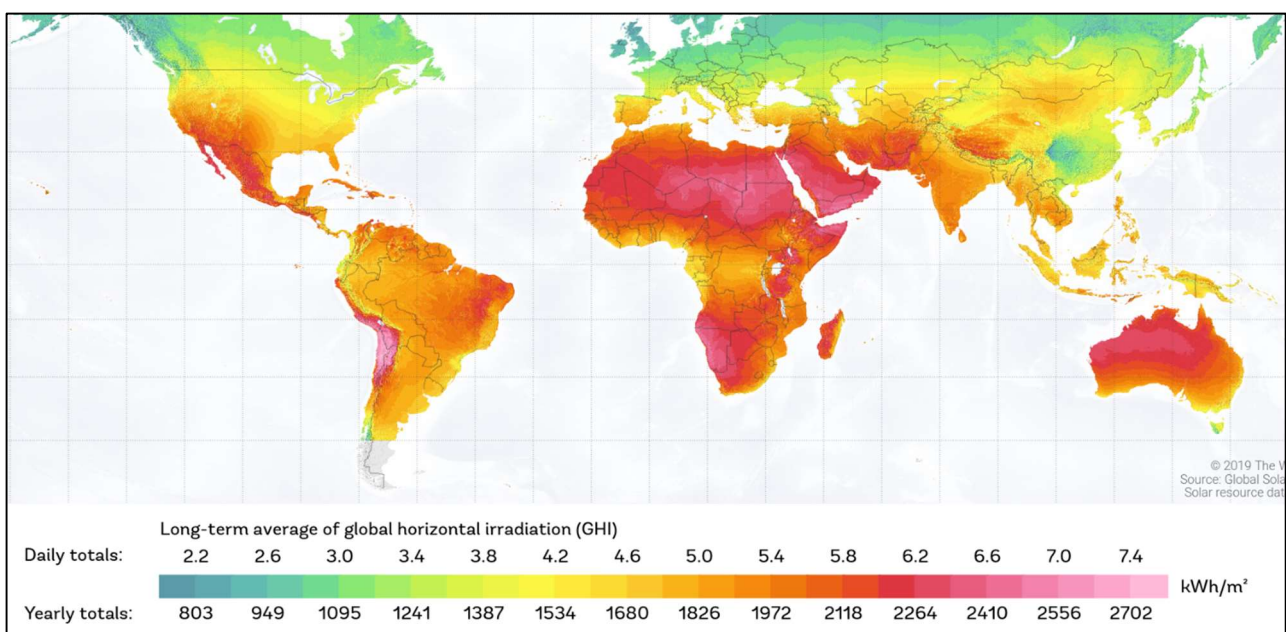


Figure 3 - Yearly average global horizontal irradiation in the world [36]

The possibility to localize the CSP plants in desertic and unexploited regions make this technology interesting. In fact, in contrast to PV, whose efficiency is affected at the high temperature reached in the desert (drops are evaluated in a range between $-0.30\%/K$ and $-0.45\%/K$) [17], CSP plants decrease their thermal dispersions in all the parts of the plant exposed to atmospheric conditions. In this way, it is possible to occupy areas that cannot be used for agriculture or other human activities.

Then, thanks to TES, it is possible to efficiently store hot fluid and decouple electricity generation. But instead of heat, it is also possible to exploit extra energy to provide other assets: for instance, if the plant is located by the sea, a solution can be the one to desalinate water to feed a local fresh water supply. [18] This process is called hybridization and other solutions consist of the production of hydrogen or of a direct use of heat for industrial productions.

3.3 The downsides of CSP

Observing the regions where CSP plants can operate, it is possible to notice that most of them is located in remote regions, far from big cities (especially Sahara or Australian desert). If this technology is perfectly suitable for a local use of electricity or other assets, but long-range electricity transport can introduce in the system non-negligible losses.

Instead, for what concern the densely populated regions like California or Andalusia, an important downside to take into account is the large land consumption. For instance, in the US, it has been estimated an average value of land consumption for CSP and photovoltaic energy production. If a PV plant can consume between $1.1 \frac{ha}{GWh/y}$ and $2.2 \frac{ha}{GWh/y}$, CSP is less spread (even though a wider variety of concentration systems), settling between $1.3 \frac{ha}{GWh/y}$ and $2.1 \frac{ha}{GWh/y}$. [19]

A good comparison for these values can be offered by another analysis, performed in the United Kingdom. The results about the land consumption are collected in a region where solar radiation is much lower due to latitude and oceanic moisture, so CSP is not feasible there. On the other hand, at the beginning of the century, photovoltaic energy has got an increasing importance in the local energy mix, even if with a smaller productivity with respect to other, sunnier places. [20] It is interesting to notice how the land consumption for nuclear power, characterized by extremely high energy density and capacity factor, amounts on average to $0.03 \frac{ha}{GWh/y}$, namely almost two orders of magnitude less than CSP in the USA. Coming to wind power, this source is strongly affected by turbulence disturbance to the wind fields so it requires an increasing spatial distancing as the size of the farm becomes larger and larger. Thus, single turbines or small farms have a moderate impact, while the largest ones require a much larger area. The values of land consumption are approximately between $0.1 \frac{ha}{GWh/y}$ and $4.3 \frac{ha}{GWh/y}$. Last interesting benchmark in this framework is biomass, which is a different energy source since it also requires soil for the production of organic material to burn: the average value of land consumption in Britain for wood and other organic fuels is about $45 \frac{ha}{GWh/y}$, namely one order of magnitude more than solar and power and more than three more than nuclear. Therefore, it is possible to infer that concentrated solar power does not suffer any additional big issues more than PV plants or even wind farms, while it gives the chance to be connected to a TES. [20]

4. The components

4.1 The typical configurations of CSP plants

The four main CSP technologies -solar tower, parabolic trough (PT), linear Fresnel (LF) and dish- are different in their principles and generally in their structure. Nevertheless, a series of common elements is always present about the system-level configuration. First, mirrors are aligned to concentrate the light onto a receiver, hence they need to be curved to reach a sufficient concentration factor depending on the requirements of the power cycle. The mirrors are handled to follow the trajectory of the sun during a day; therefore, a control system which takes care of the proper alignment is necessary for the support structure of the collector. The hot fluid produced may directly feed a heat engine, it may transfer the heat to a secondary cycle or it may be stored in a tank for a latter exploitation. [21]

4.2 The collectors

The main concept at the base of CSP plants is concentrating the direct solar irradiation on a proper receiver that transfers the solar energy to a heat transfer fluid. The key parameter for a simple evaluation of the performance of a CSP collector is the concentration ratio (CR), which is the ratio between the areas on which the solar power is collected and the one on which it is reflected.

Four concentrator solutions have been proposed during the years, classified as punctual or linear. The first category is characterized by mirrors that focus light on a point located in front of their plane, by tracking the sun position through the mirror rotation on two axes. Solar towers and dishes take make use of this technology, exploiting larger concentration ratios and higher temperatures on the receiver.

Instead, linear collectors consist of parabolic or slightly curved mirrors that concentrate sun rays on a pipe set on top of them. The solar fields are composed by a series of straight lines in parallel in which the HTF flows and it is progressively heated. Plants adopting parabolic troughs and linear Fresnel concentrators are based on this concept: despite a smaller CR due to a less efficient tracking system, they are interesting thanks to their simplicity and lower investment costs.

4.2.1 Solar dishes

This group of concentrators allow to focus the sun radiation on a focal point set right in front of the mirrors, where the receiver is located. The concentrator tracks the sun (two-axis tracking system) to keep the incoming solar rays perpendicular to the aperture area.

As shown in the Figure 4, the receiver is usually equipped with a small turbine or a Stirling machine, both capable of directly operate the thermodynamic cycle with the atmospheric air or with helium. In the first case, the HTF is directly absorbed and released in the ambient, while in the second a closed loop is inserted. Stirling machines are preferred because of their better efficiency: this design eliminates the need for an intermediate loop or a cooling system and, enhancing the thermodynamic performance. [12]

On the other hand, the fact that almost these devices are not physically large enough to make possible a coupling to any significant storage, makes this solution more similar to a PV, also because of the average size (some kW). In fact, solar dishes compose a small fraction of the market and it is not used for large-scale applications. The real, future interest of such technology consists of the extreme temperatures that it is possible to reach on the receiver surface, which can be useful for a wide variety of applications. In general, since dish/engine systems are not yet a mature technology, an assessment of their performance is currently limited to prototype testing for research. [12] [21]

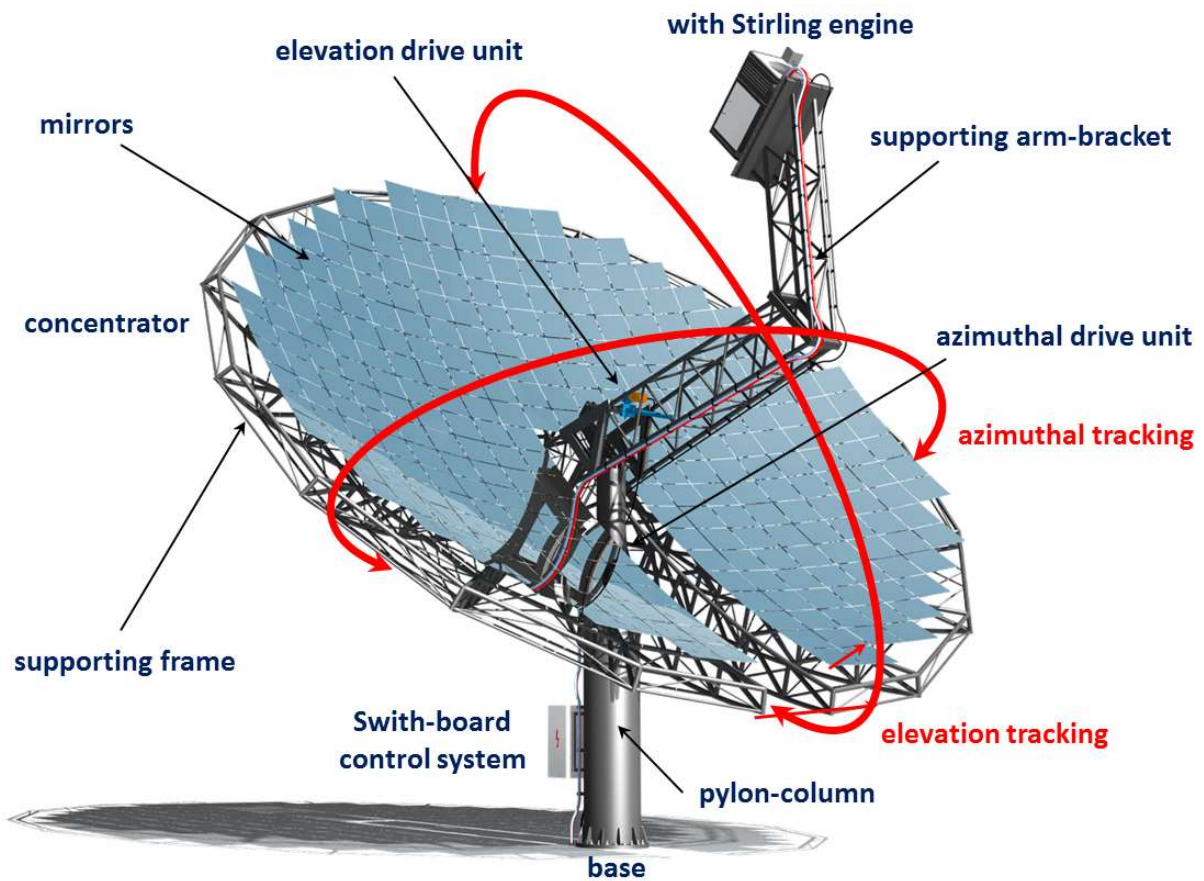


Figure 4 - Components of a typical solar dish [37]

4.2.2 Solar towers

The solar tower technology consists of a large heliostat field that includes hundreds of mirrors, which concentrate the solar radiation on a receiver located on the top of a high tower. This technology allows reaching very high temperatures ($> 800\text{ }^{\circ}\text{C}$) improving in this way the efficiency of the thermodynamic cycle downstream the receiver. As for dishes, this type of plant is technologically interesting because of the extremely high temperatures that it is possible to obtain. [12]



Figure 5 - An example of a 10 MW solar-tower plant at Shouhang, China [40]

In tower applications, mirrors are required to reflect the sunlight from the field onto the tower, working as receiver. The arrangement of the solar field and the manufacturing of the mirrors is tricky, because of several technical issues. The reflector is typically of a size of $\sim 2 \div 180 \text{ m}^2$ [22] and it is attached to a back structure, mostly of a metal framework. Since the mirror size is limited by the manufacturing and handling process, larger mirror areas have to be composed from individual mirror facets. This alignment process, necessary not to create overlapping images on the receiver, is called “canting”. In addition, in order to reach the highest concentration, each facet must be curved according to the distance between heliostat and tower. [21]

The typical HTFs of solar-towers plants are steam and molten salt. Whenever these fluids are used, for which high temperatures are required, the receiver surface is made of steel and it is either uncoated or painted black. [21] The absorptance of such devices is reported to be close to 90%, even taking into account the onset of an oxidation layer on the uncoated metal surfaces. [23] The high temperature that is generally reached on the surface of the receiver is responsible for a series of non-negligible losses: in addition to reflectance and re-emission losses, the elevated altitudes of the towers expose them to a strong convective cooling by wind. [21]

4.2.3 Parabolic trough

In parabolic trough systems, mirrors are aligned along the axis of the support structure. The fact that the concentration ratio is smaller for parabolic trough (as well as linear Fresnel, as a line-focusing collector) is due to the shape of the mirrors itself, whose area is naturally limited. The typical configuration of such solution consists of the assembly of some differently shaped mirror facet, exploiting the symmetry of the curve. They concentrate the radiation in a focal line where a pipe, working as a receiver, is located. Hence, tracking is only possible in one axis. [21]

The absorber tube is composed by a precise series of materials. A thin stainless-steel tube is the place where the fluid flows, surrounded by a vacuum annulus encapsulated into a borosilicate glass layer. The introduction of these materials is justified by the maximization of the thermal resistance and the minimization of the radiation buffering of a non-transparent coating. The heat loss increases exponentially with the absorber temperature [21]

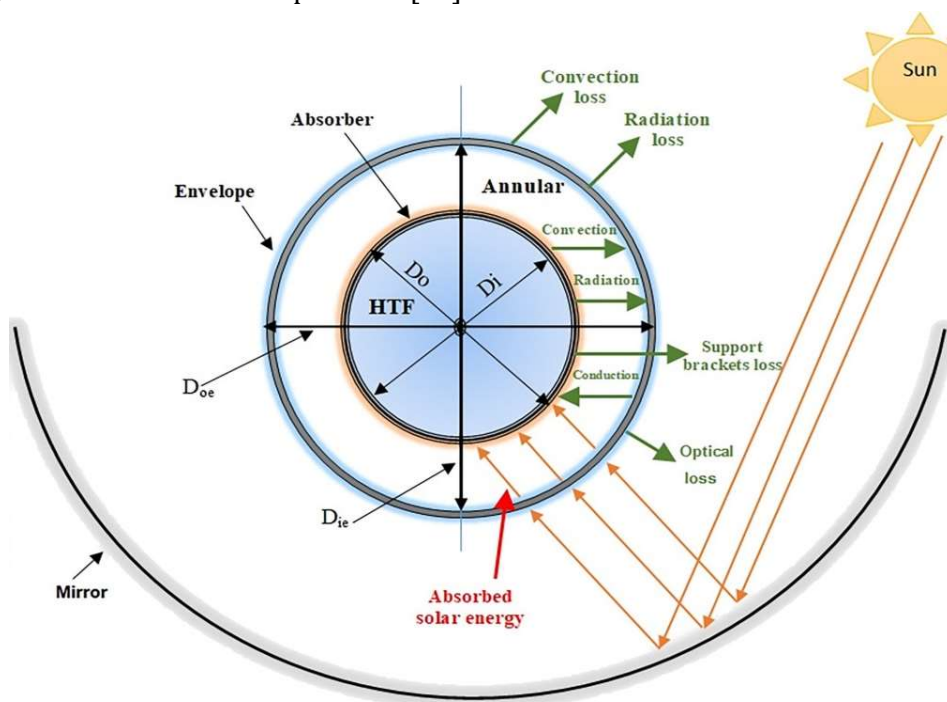


Figure 6 – The receiver cross section of a PT plant and the power terms involved [41]

Parabolic troughs represent the vast majority of the current commercial plants since they are the most mature technology. For the future, it is forecasted to see a great fraction of this features but not a dramatical engineering enhancements. [12]



Figure 7 - A photo of a parabolic trough [39]

4.2.4 Linear Fresnel Collectors

The linear Fresnel Reflector (LFR) system consists of a set of parallel mirrors strips having (typically) a slight curvature that aim at reproducing the optical behavior of a parabolic mirror like that used in the PT systems, despite worse optical efficiencies. Plane mirrors suffer from too high optical losses therefore mirrors are usually one-axially curved by gluing them on a slightly curved support structure. [21]

The sun light is reflected onto an absorber tube that is cooled by a heat transfer fluid that flows inside. Given that the concept of the receiver is the same of the PT collectors, the structure of the pipe typically the same. In general, LFRs is considered a promising technology because of the simplest solar field compared to PT system, that leads to a cost reduction. [12]



Figure 8 - A photo of a LFR [42]

In some setup like the one shown in the Figure 9, it is possible to observe the presence of a secondary reflector, namely a mirror located behind the absorber tube, with the view to recover a part of the sunlight reflected in the wrong direction.

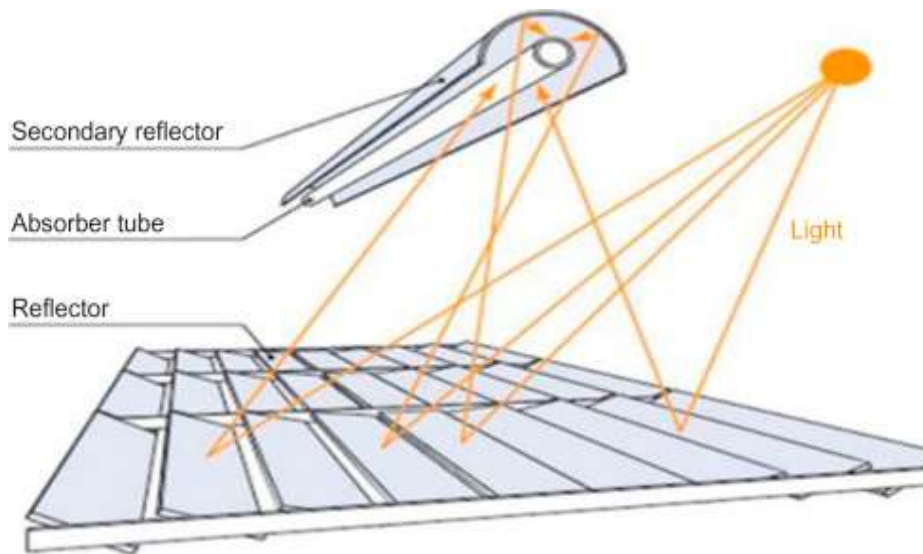


Figure 9 - A sketch of a LRF equipped with secondary reflector

4.3 The heat transfer fluids

Because of a large series of technical constrains that CSP plants involve, only a small number of heat transfer fluids is actually adopted in commercial systems. Line-concentrating plants usually make use of mineral oil, but sometimes solar salt is preferred. Moreover, it is possible to find plants using steam.

The first compound is a synthetic high temperature oil, capable of safely work until 400°C. This value is not as high as the one that other HTFs can withstand and it is not capable of provide a sufficiently high thermal efficiency; hence the plants are kept as close as possible to the limit, exposing the oil to risks of decomposition and wear. The gaseous phase generated by the oil overheated needs to be separated by a proper system in order to avoid a worsening of the thermal performance of the receiver. Thus, the mineral oil properties need to be continuously monitored throughout the lifetime of the plant. [21]

The second HTF is solar salt. Also called molten salt, it is an eutectic mixture of 40% KNO₃ and 60% NaNO₃, capable of safely operate in a range of 260 ÷ 550°C. Its non-flammability and non-toxicity, together with good thermal properties at a relatively low cost make this solution particular interesting. Finally, its small density variation at the phase change (~4.6%) prevents structural damages in the case of freezing; a dynamic control is anyway continuously operating to avoid the freezing. [24] On the other hand, in plants adopting solar salt need to be monitored due to the possible damages of corrosion, which can affect the components lifetime. [21]

A last HTF adopted in tower plants is superheated steam, which allows to only use a fluid for both the solar and the power block. Despite this undeniable positive aspect, it is losing attractiveness because of simplification and avoided costs for the heat exchangers between receiver and storage in molten salt systems. However, the storage of steam is much less efficient. [21]

4.4 The storage systems

One of the main strengths of CSP plants is the capability of storing energy, which then can be delivered with a dispatchable regime, obtaining a larger economical gain. In the absence of storage, on the sunniest hours, plant operators would need to “defocus” some unneeded solar collectors to maintain a stable electricity output regime. Storage avoids losing this energy and it allows to extend production after sunset. [12]

The natural technological solution for this purpose consists of thermal energy storage (TES) because it allows to directly accumulate heat, which can be converted into electricity in a later time. The forms in which thermal energy can be stored are three: sensible heat (SHS), latent heat (LHS) and thermochemical heat storage (TCS). Whilst SHS systems allow to store energy by a temperature increase, LHS devices make use of the latent heat characterizing the phase-change materials (PCM). TCS systems, instead, store energy by means of endothermic chemical reactions, and the energy can be retrieved by facilitating the reverse, exothermic reaction. [25] [26] [27] [28]

Thermochemical heat storage systems are emerging as a potential energy storage solution thanks to their superior energy density and to the absence of energy leakage throughout the technology storage duration. They are still at a laboratory stage. [26]

4.4.1 The sensible heat storage

This SHS represents the simplest solution and the most widespread, even if it is generally characterized by a relatively low energy density. [26]

Within the several technologies for SHS, it is possible to split two groups on the base of the medium adopted: fluid, namely the most widespread in the CSP framework, or solid medium. The first solutions are simpler to implement because, thanks to the pump, it is possible to handle and store the fluid in tanks. Instead, the management of solid materials is not equally easy. [26] Indeed, at the state-of-the-art, the largest part of SHS systems make use of solutions which belong to the first group. [28]

In parallel, it is possible to classify the SHS systems on the base of how energy is delivered to the storage. In particular, if the fluid is directly introduced into a tank or a proper device, the storage is called direct; this is the case of steam accumulators or molten salt tanks. Reversely, if an intermediate loop is necessary, the storage is named “direct”.

As mentioned above, in the context of CSP, the most widespread solutions consist of liquid medium storage technologies. Specifically, the most common solution is the two-tank molten salt storage. [28] Basically, the volumes of hot and cold salt are maintained in separate reservoirs. The storage system is charged by introducing excess heated HTF to the hot tank from the cold tank; later, to discharge the storage system, the process is reversed with the stored heat being transferred to the power block. [25] This solution can claim a relatively high energy density, a simple operability and it is compatible to both mineral oil (through its indirect configuration) and with molten salt (direct).

Alternatively, the other prevailing technology is composed by thermocline tanks. They consist of reservoirs in which a constant thermal stratification is maintained through strong buoyancy forces, driven by the density differences. As a result, hot and cold fluid do not mix. A low-cost solid filler material fills much of the device to displace the higher cost HTF and act as the primary thermal storage medium. The layers in which a temperature gradient is evident is thin. The presence of a single tank ensures a less efficient storage, but also lower investment costs. [25]

Finally, steam accumulators are the solution adopted in the solar tower plants which make use of superheated steam as HTF. The main difference to molten salt tanks lies in the fact that instead of a liquid, the tank is filled with a gaseous element. As a consequence, pressure variation during the discharge and leakage make steam accumulators a less efficient solution. [28]

4.4.2 The latent heat storage

The latent heat storage systems are the first alternative to SHS ones since they can claim higher energy density. On the other hand, their handling is trickier because of complicated by moving phase change boundaries. [26]

They can make use of several media. Within phase-change materials it is possible to find:

- Organic materials, such as paraffin, fatty acids, esters, alcohols and esters.
- Inorganic materials, like salts (mainly NaCl), salt hydrates and metals.
- Eutectic mixtures.

In general, all these solutions have not yet been demonstrated at a commercial scale. [29]

4.5 The backup systems

An option able to improve the flexibility of a CSP system is to include a backup system, namely a fossil-fuel heater that provides thermal power to the system on demand in order to keep a constant output also in the case of a long absence of sun or not to let the hot tank fluid temperature fall. An example of the contribution that a backup heat may give is shown in Figure 10.

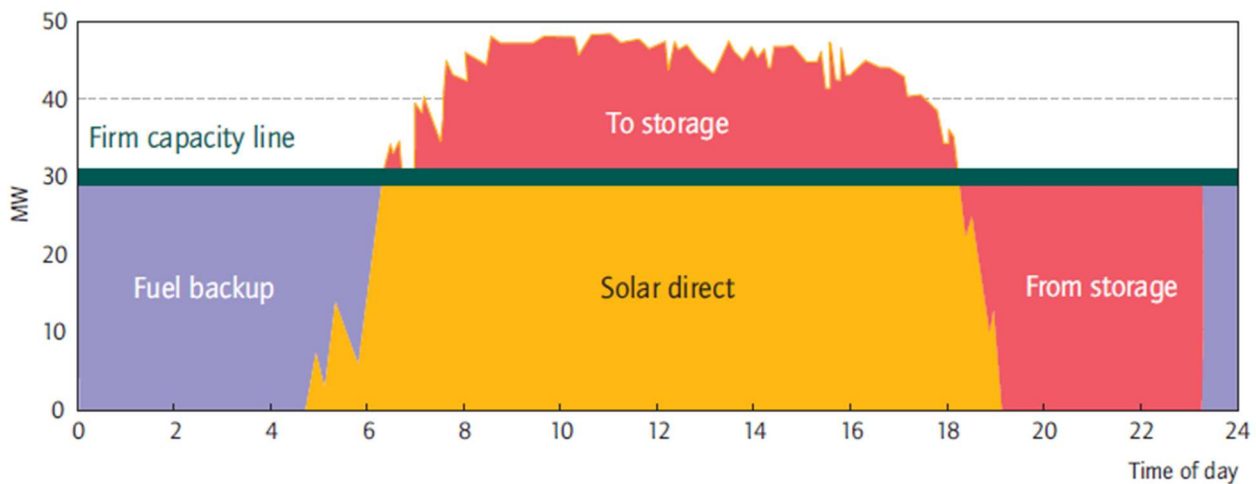


Figure 10 - An example of the backup introduction in a CSP plant [12]

Commercial CSP plants usually incorporate auxiliary boilers that are used to supplement the solar input during the night and during periods of low solar load. In parallel, this backup energy is also required to avoid freezing of the HTF at night and to allow quick daily start-up operations. [30] The thermal power supplied needs to be regulated in time, for a correct load management. A refined adjustment is possible through a natural gas burner, which is quick to reach the regime state. The heated HTF, then, get to the steam generator to produce electricity in the turbine.

Finally, integrated solar combined cycle systems (ISCCS) are a solution to hybridize a CSP plants. As well as combined cycle plants, the ISCCS configuration allow to use the waste heat of a gas turbine to feed a Rankine cycle, also driven by a CSP plant. Thanks to the flexibility of the gas turbine, it is possible to maintain a constant electricity output at the steam turbine, compensating the intermittence of the CSP thermal output. [31]

5. The reference plant

5.1 The plant

The aim of the present thesis is to develop a system-level model of a CSP plant based on the linear Fresnel technology. The reference plant is the Partanna CSP plant, commissioned by FATA E.P.C., in Sicily, Italy. The data about the reference plant have been kindly provided by the FATA E.P.C company, which however cannot be disseminate here.

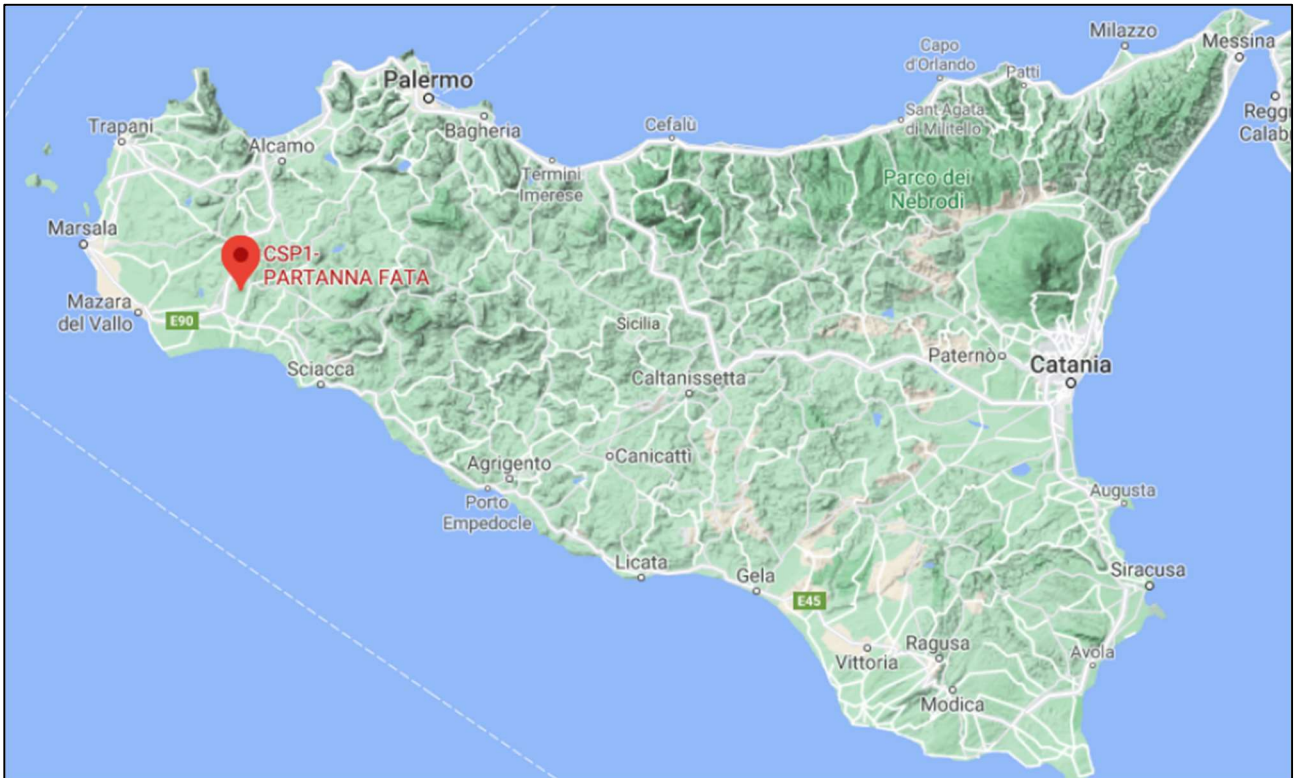


Figure 11 - Geographical position of the plant [38]

The solar salt is adopted as heat transfer fluid, because it is capable of safely operate in a range of $260 \div 550^{\circ}\text{C}$. The main advantage that comes from the choice of this fluid consists of the elimination of an intermediate loop for a HTF, whose task is directly performed by the molten salt itself. Hence, the only heat exchanger is a steam generator fed by the heat received either in the solar block or in the backup.

Macroscopically, the system is composed by few blocks, where energy is transformed, stored or transferred. The primary loop is the molten salts loop, which includes the linear receiver, the storage unit (two-tank configuration), the backup unit (gas-fired heater) and the steam generator. The latter allows transferring the heat gained by the salts to the secondary loop, which corresponds to the power block, namely a Rankine cycle capable of converting the thermal power into electricity for the grid. In the Figure 12 it is possible to see the scheme of the plant, in which all the possible connections among elements are reported.

Since the direct normal irradiation (DNI) changes during the day, the molten salts mass flow rate flowing in the receiver is controlled in order to keep the salts temperature at the outlet almost constant (550°C). The mass flow rate of molten salts in the steam generator is also regulated depending on the desired electricity output. The flexibility is limited, though: the Italian electricity service management imposes a maximum percentage of electricity generation by gas combustion at 15%.

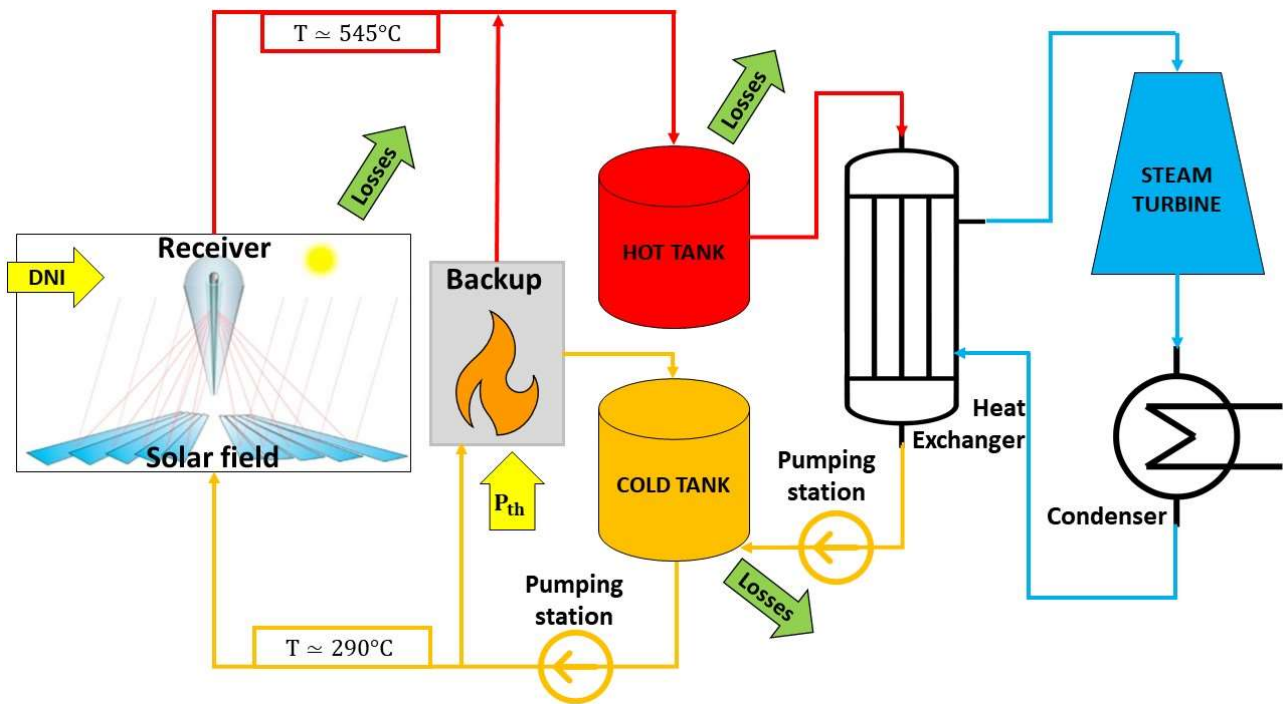


Figure 12 – Partanna plant scheme

5.2 The two-tank storage

The tanks where molten salt is stored are a complex system, capable of interfacing with the other components through several plugs. The stratigraphy of the walls is composed by a first metal layer with a structural purpose, an isolation coat made of Pyrogel XT and another external thin metal film not to expose the isolator to the external weather conditions. The thickness of the intermediate layer depends on the salts temperature in the tank, the hotter the salts the thicker the insulation layer. The side and the top walls are exposed to the ambient air, while the bottom side is placed on the concrete basement under which a series of channels allows an air flow to remove the heat and to prevent its degradation.

The heat losses affecting the storage thermal performance are due to the convection and radiation occurring from the external surfaces exposed to the environment and by conduction towards the ground on the bottom side. The tank breathing involves the continuous absorption of fresh air during discharges and waste of hot air during charges.

5.3 The pumping stations

The pumping system is composed by two stations: the first is used to feed the line composed by the solar block and the backup, catching from the CT; instead, the second station leads the heat transfer fluid to the heat exchanger from the HT. It is fundamental to underline that the solar field is located on a hill and most of the energy necessary to pump the salt across the plant is used to overcome such a head.

The typical operations involving the plant management are four. The direct solar energy collection by forcing the cold salt to cross the solar field is the main procedure, but sometimes it is sent to the backup burner to prevent a temperature drop in the HT during cold or cloudy periods. However, the control system continuously monitors the CT temperature in order to avoid freezing and to do it, a flow rate is sent to the backup burner and then re-injected into the cold tank. Finally, a minimum anti-freezing flow rate is always pumped across the boiler, when it is not working, and the field, at night.

5.4 The solar field

The project is focused on the modeling of an auxiliary system of a linear CSP plants. Hence, it is possible to couple it with a linear Fresnel (like for the case of the plant at Partanna) or a parabolic trough system, supposing to collapse it into a solar block with an input and an output manifold, delivering the heated fluid from the CT to its destination. The solar block can be split into the solar mirrors and the pipe onto rays are concentrated.

6. The system-level model

The Modelica language [32] is adopted to develop the system-level model of the Partanna plant. Modelica is an a-causal, object-oriented language that allows modeling the plant components and subcomponents, which are then combined to simulate the whole system.

6.1 The storage

Due to the complexity of the system, this feature is composed by a series of sub-models. No distinction has been made between CT and HT since the only differences are the salt temperature (computed by the model) and the dimensions, which can be varied in the model.

The general modeling strategy has been inspired and based on the Zaversky paper [33], adjusted to the Partanna plant, according to FATA guidelines. The model solves the dynamic mass and energy balance in the molten salts and in the air layer above the salts, while a steady momentum balance equation is introduced that simply impose the hydrostatic pressure at the salt inlet and outlet ports. The dynamic energy balance equation is solved in the solid structures composing the walls and proper correlations are used to quantify the heat transfer coefficients of fluids on them.

The main assumptions introduced are:

- The curvature of the top wall has been neglected assuming, for the sake of simplicity, that it is a flat surface.
- No stratification is considered: the thermal state of the tanks is evaluated by a bulk temperature, expression of a 0D model.
- The air above the molten salts is transparent to the thermal radiation.
- The solar load on the outer face of the tanks is neglected.
- The ground below the concrete basement, used for structural purpose, is at the ambient temperature.
- Across the walls, only a 1D temperature distribution in the normal direction is evaluated.

The summarizes the heat transfer phenomena considered in the model are shown in the Figure 13.

6.1.1 The molten salt stored

The base component is related to the molten salt contained in the tank, which is thought to dynamically compute the fluid level (determining the mass stored) and temperature, as a response to the external conditions. The model is provided with multi-inlet/outlet ports of molten salts, in order to connect the storage model with the rest of the circuit. A 0-dimensional approach has been chosen for the simulation of this model, because it is not expected to observe a substantial stratification along the tank axial or radial direction.

$$\frac{d}{dt}(M(t)) = \sum_{ports} G_i \quad (1)$$

$$\frac{d}{dt}(M(t) h(t)) = \sum_i^{ports} G_i h_i - Q_{bottom}^{conv} - Q_{side}^{conv} - Q_{gas}^{conv} - Q_{roof}^{rad} \quad (2)$$

$$p_i = p_{amb} + g \rho H(t) \quad (3)$$

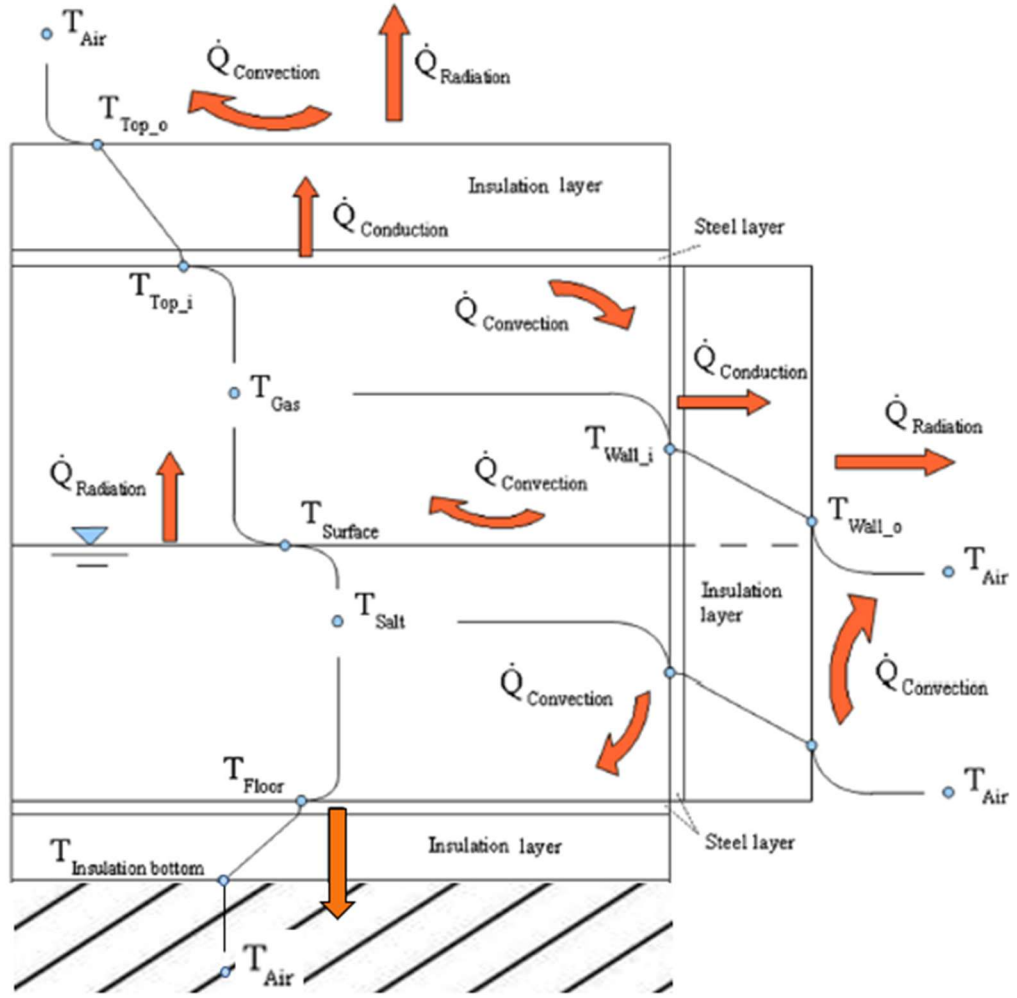


Figure 13 - The heat transfer phenomena considered in the model [33]

As mentioned above, the model solves the dynamic mass (eq. (1)) and energy (eq. (2)) equations. In the first (1), M stands for the mass of the stored molten salt, while G represents the mass flow rate of the i -th port of the tank. Then, in the second (2), the enthalpy h of the bulk fluid is evaluated and it provides the values of temperature of the fluid, taking into account the introduction into the system of a variable number of mass flow rates G_i through the ports characterized by an own enthalpy, h_i and the series of terms of the power dispersions. Finally, the third equation (3) shows the imposition of the hydrostatic pressure p_i at the salt inlet and outlet ports.

The heat transfer mechanisms that lower the salts temperature in the tank are the natural convection (bottom/side wall and air layer above the salts) and the radiation transferred from the salts free surface and the top wall of the tank. The effect of the salts inflow/outflow is very negligible, i.e., it does not induce an additional movement of the stored salts that potentially can affect the convective heat losses.

In order to compute the convective heat transfer, a proper convective heat transfer coefficient has to be introduced. On the side wall, which compose the largest part of the dispersion due to its larger surface, a correlation suitable (4) for vertical plates has been used to calculate the heat transfer coefficient. [34]

$$\begin{cases} Nu = 0.68 \frac{Pr_{film}^{0.5} Gr_{film}^{0.25}}{(0.952 + Pr)^{0.25}} & \text{if } Gr < 10^9 \\ Nu = 0.13 (Gr_{film} Pr_{film})^{\frac{1}{3}} & \text{if } Gr > 10^9 \end{cases} \quad (4)$$

Instead, for the horizontal interfaces, in terms of bottom and upper free surface facing the gas, a horizontal plate correlation was proposed. This is dependent on the orientation of the plate:

respectively, the first correlation (5) was used for the convective coefficient to the gas, while the second (6) for the one to the bottom. [34]

$$Nu = 0.27 Ra_{film}^{1/4} \quad (5)$$

$$\begin{cases} Nu = 0.54 Ra_{film}^{1/4} & \text{if } Ra < 10^7 \\ Nu = 0.15 Ra_{film}^{1/3} & \text{if } Ra > 10^7 \end{cases} \quad (6)$$

Finally, radiative heat transfer between the salts free surface and the top wall of the tank is computed according to the Stefan Boltzmann law. A proper correlation (7) about the view factor for the inner faces of a cylinder with a variable fluid level is used. The gas is supposed to be completely transparent to the radiation. [33]

$$F_{form}(t) = H(t)^2 + 2R_{cyl}^2 - \frac{\sqrt{(H(t)^2 + 2R_{cyl}^2)^2 - 4R_{cyl}^2}}{2R_{cyl}^2} \quad (7)$$

6.1.2 The air layer

The concept of the heat transfer modeling of the gas medium is the same for the liquid, since the mass stored is subject to a strong variability. It is fundamental to highlight the fact that instead of receiving fluid coming from other blocks, as for the molten salt, during discharge air is directly sucked from the ambient. However, the small mass contained and the low specific heat of air would lead to a very small thermal inertia during transients.

$$\frac{d}{dt}(M(t) h(t)) = +Q_{liquid}^{conv} \pm G_{ext} h_{ext} - Q_{top}^{conv} - Q_{side}^{conv} \quad (8)$$

As for the one concerning the stored molten salt, this model solves the dynamic energy equation (7): again, the mass of the system is expressed by the variable M and its enthalpy h is then translated into the temperature of the bulk air. The three convective terms represent the possible heat transfer mechanisms: the gas can be heated by the molten salt (which works as an energy source) and then it releases heat to the interfacing walls, namely the top and side ones.

The air mass value is driven by the volume of molten salt, whose level is communicated to this model through a proper connector. The variation of the level is translated into the flow rate value G_{ext} mentioned in the equation (8).

The correlations are the same used in the stored-molten salt model. [34]

6.1.3 The walls

As mentioned above, the walls of the tanks are composed by a series of three materials, playing different, complementary roles. The thermal conduction is assumed to occur only in the direction of the wall thickness since the temperature of the air is expected to be close to the molten salt one and no stratification phenomena is taken into account. Moreover, the presence of any possible thermal bridges is neglected.

The inner metal layer, few centimeters thick, is used for structural purpose and to face a corrosive fluid; the chosen material is stainless steel AISI 316. It has been modeled by considering one volume (in which properties are evaluated) for which the dynamic heat transfer equation (9) has been solved. On the

internal face, the temperature T_{int} is imposed equal to the one of the molten salt (10), while on the outer, the same is done using the internal temperature, defined as T_{ext} , of the isolation layer (11). Hence, the metal layer works as a single thermal resistance.

$$\rho c_p \frac{dT_{wall}}{dt} V_{wall} = Q_{in} - Q_{out} \quad (9)$$

$$Q_{in} = \frac{T_{int} - T_{wall}}{R_{th}} \quad (10)$$

$$Q_{out} = \frac{T_{wall} - T_{ext}}{R_{th}} \quad (11)$$

The thermal resistance is evaluated applying the analytical conduction equation in radial coordinated for the lateral side, introducing the logarithmic coefficient. Instead, for what concerns horizontal plates, the temperature distribution is linear in the transversal direction. For the vertical wall, the power released on the internal face, Q_{in} , is the sum of the molten salt and air contribution, while on the ceiling of the tank Q_{in} is the addition of the liquid radiative and of the gas convective contributions.

The other layer composing the wall is the Pyrogel XT isolation. It needs to be the key element in the chain to assure a small transmittance through the wall. The differential equations describing the conduction mechanism are the same, but reverse: indeed, the imposition of a Robin boundary condition (including both a radiative and a convective mechanism) is performed on the outer surface, while on the area in contact with the steel layer the two materials are supposed to have the same temperature.

As a consequence, the temperature distribution on the flat plates (roof and bottom coatings) result to be linear, so they are collapsed into a simple resistance. Instead, the cylindrical wall shows a logarithmic shape of the temperature, which is evaluated through a finite-volumes split by the equation (12).

$$Q_i = \frac{k_i + k_{i-1}}{2} (2\pi r_i) H_{roof} \frac{T_{i-1} - T_i}{\log \frac{r_{i+1}}{r_i}} \quad (12)$$

The external metal sheet is not modeled because of its negligible thermal resistance. Its only contribution is indirect: in the daytime the same irradiation deposited on the solar field reaches the tanks, heating them. This contribution is undoubtedly irrelevant compared to the other powers involved, especially since the external, metal sheet tends to reflect more than a half of the incident solar energy. Hence, also this term has been neglected.

6.1.4 The system-tank

In the Figure 14 **Error! Reference source not found.**, the system-level assembly is reported. It is composed by two images, marked with two stickers: in the number 1, a zoom shows the coupling of the air and molten salt models, which once together constitute a sub-model for the general tank structure, reported in the figure number 2.

In the sub-model the connectors are evident, because it is possible to observe the two collected ports for the power exchange with the side wall, the two with the top and the one with the bottom. In the external model, these three lines find the metal and isolation layers of the walls as thermal resistances in series. At the end of the top and side wall lines, a model capable of imposing the external boundary conditions is set, while at the bottom, the value of ambient temperature is forced.

The model requires the initial conditions (in terms of filling percentage of the tank and bulk solar salt temperature) and the tank dimensions. The time-dependent ambient temperature and wind speed has to be provided to define the boundary conditions.

The model of the tank can also be used for other purposes since the media can be changed through the control panel as well as the tank dimensions.

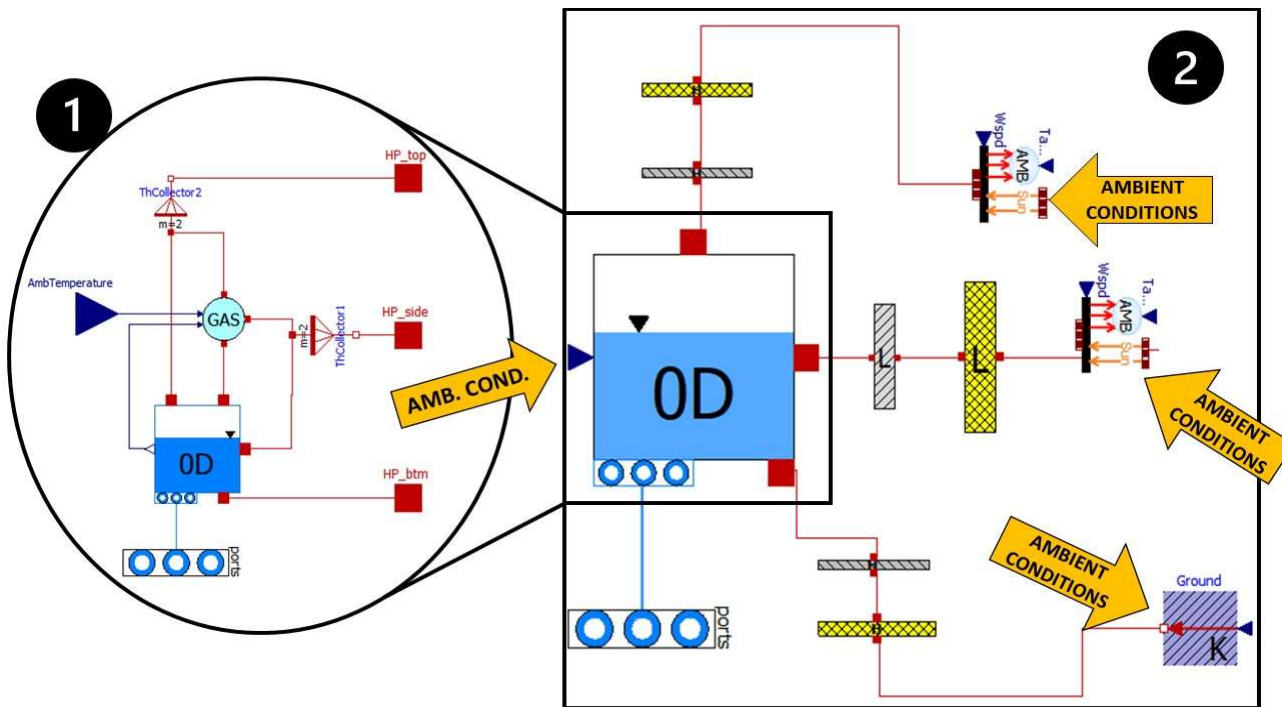


Figure 14 - All the components of system-tank model

6.1.5 A tank performance verification

As reported by Fritz Zaversky et al. in the reference paper for the modeling of the tanks, storage systems for commercial parabolic trough collector plant typically experience a decrease for the hot and the cold full tank of less than 1°C per day, and 5÷6°C at the minimum molten salt level [33]. This information is used as a benchmark for our results, performing tests with likely external condition with no fluid exchange across the ports.

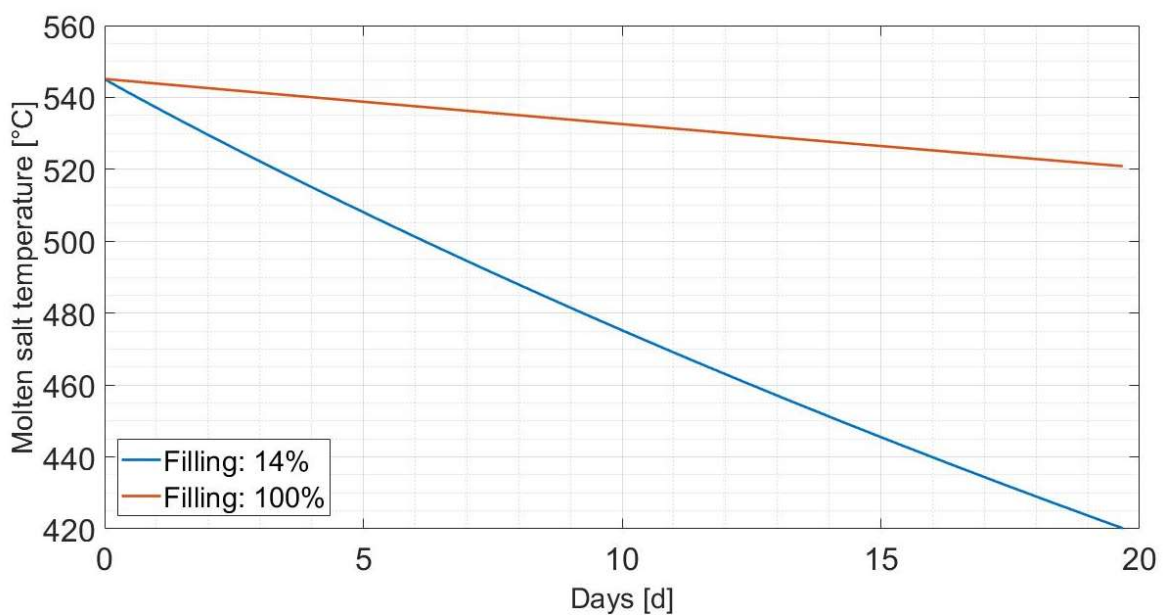


Figure 15 - The temperature evolution got as results of the simulations

In the Figure 15, the comparison between two possible cases of the hot tank is reported. In the first, the plant is left at rest with an around 15% filling percentage and the bulk temperature of the stored molten salt is observed for twenty days. What is observed was an overall 130°C loss corresponding to a $\sim 6.5^\circ\text{C}/d$, namely an acceptable result if matched with the benchmark. In the second case, the HT has been filled until 100% and then left cool down under the same meteorological conditions. Again the 25°C loss result is satisfactory because coherent to a $\sim 1^\circ\text{C}/d$ drop described by the benchmark.

The molten salt cooling is due to the sum of contributions discussed among the modeling strategies. For both conditions, the 81% of the power loss is due to dissipation through the lateral wall, 11% through the bottom, 5% is due to radiation to the roof and 3% is released to the air (which than heats the side wall on the uncovered surface). Such a combination was expectable since the molten salt is notably a good heat transfer fluid, so it easily releases heat by conduction, especially on a large wetted surface ($26 \div 326 \text{ m}^2$). At the same time, the poor thermodynamic performance explains the small heat exchange at the interface between the two fluids.

Thus, it is possible to use these values as a sanity check of the tank model in steady conditions.

6.2 The backup heater

The base concept lays in the presence of two ports, inlet and outlet, and of a coefficient reporting the working condition (in percentage) of the boiler, with a view to its regulation. The presence of localized and distributed losses, unavoidable in an intricate system like a shell and tube heat exchanger, are concentrated into a localized pressure drop.

The parameters for this model are the minimal and maximal power at which the burner is requested to work, the lower heat value of the fuel and the pressure drop it involves. As results this backup model provides the gas consumption for each operation condition and the outlet temperature of the molten salt.

The backup model has been developed as a volume in which a mass flow rate is introduced, heated and removed. The equations applied are the ones about energy (13), mass (14) and momentum (15) balances, in which G stands for the inlet and outlet mass flow rates, h for the enthalpy, Q for the energy provided by the boiler, p for the pressures.

$$G (h_{out} - h_{in}) = Q \quad (13)$$

$$G_{in} = G_{out} = G \quad (14)$$

$$p_{in} - p_{out} = \Delta p \quad (15)$$

6.3 The pumping system

For the pumping system, a couple of pumps called "*ControlledPump*" contained in the Modelica standard library [32] has been chosen. One pump forces the fluid to flow from the HT to the CT through the power block, while the other can feed both the gas-fired burner and the solar block. They take as inputs the nominal conditions (head, shaft rotational speed and mass flow rate) and they can be connected with a set of variable mass flow rates or heads it is prescribed to work.

The company FATA E.P.C. provided a series of data sheets regarding the June 9, 2015, including the mass flow rate chart and the meteorological data. Hence, such information result to be suitable for this device to drive its regulation.

6.4 The power block

The power block development is out of the scope of this thesis, but a simplified version has been created in order to simulate the presence of a power sink in the plant. The concept is the same of the backup one, but instead of the regulation of the working percentage a value for the energy extracted has to be provided.

In the same way as for the backup heater, the power block model has been developed as a volume in which a mass flow rate is introduced, cooled and extracted. The equations applied are the ones about energy (13), mass (14) and momentum (15) balances, in which G stands for the inlet and outlet mass flow rates, h for the enthalpy, Q for the energy removed by the boiler, p for the pressures.

$$G (h_{out} - h_{in}) = -Q_{rem} \quad (16)$$

$$G_{in} = G_{out} = G \quad (17)$$

$$p_{in} - p_{out} = \Delta p \quad (18)$$

6.5 The solar block

As for the power block, also the solar block is out of the scope of this thesis. The solar block model has been previously developed at Politecnico di Torino using the Modelica language. This model includes the linear receiver (an encapsulated and evacuated absorber tube) and the solar field and it determines the salts enthalpy increase given the salts mass flow rate and temperature at the inlet as well as the time evolution of the ambient temperature, wind speed and direct normal irradiation (DNI). For the scope of this work, the model parameters (solar field and receiver dimensions and materials) have been set according to the Partanna data.

7. The simulations

7.1 The framework

The models in the context of this thesis were developed for the purpose of a system-level simulation, focusing on a reliable and stable working condition of the plant. The nature of CSP involves the presence of strong oscillations of the energy source during the day and this is at odds with a steady state operation. Thus, for the simulation a reference day has been chosen to run simulations and observe the dynamic behavior of the components.

As mentioned above, the chosen day is June 9, 2015, namely a summer day with a slight but irregular cloud covering. As input for the models, meteorological data has been collected and used to the best match the natural conditions. In the Figure 16, Figure 17 and Figure 18, their trends are reported.

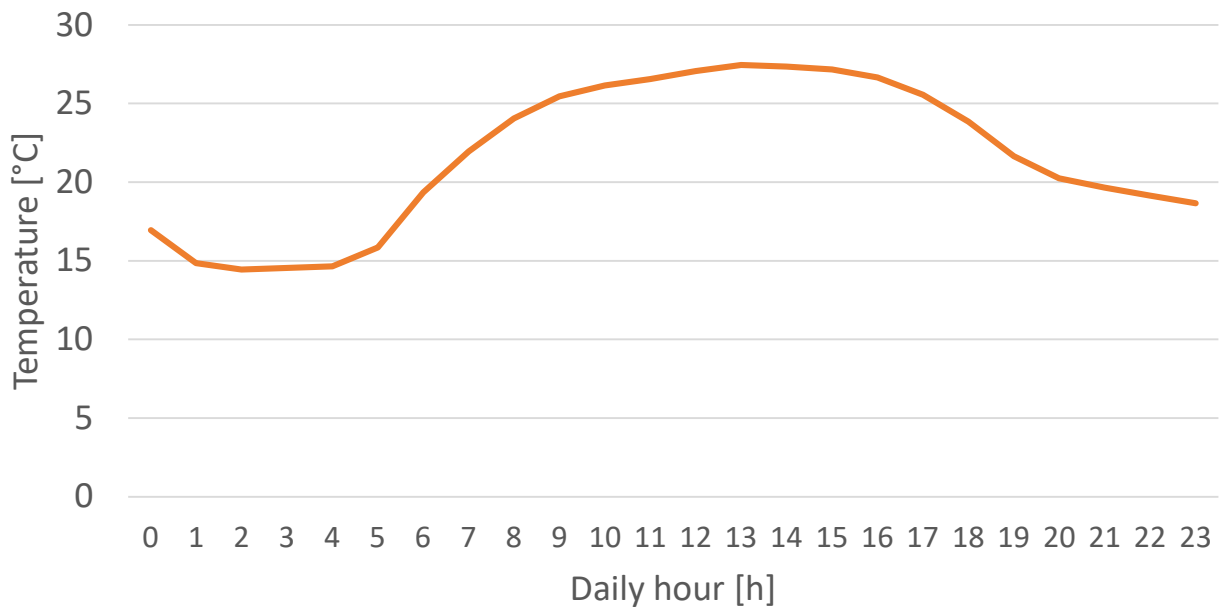


Figure 17 - The ambient temperature trend during June 9, 2015

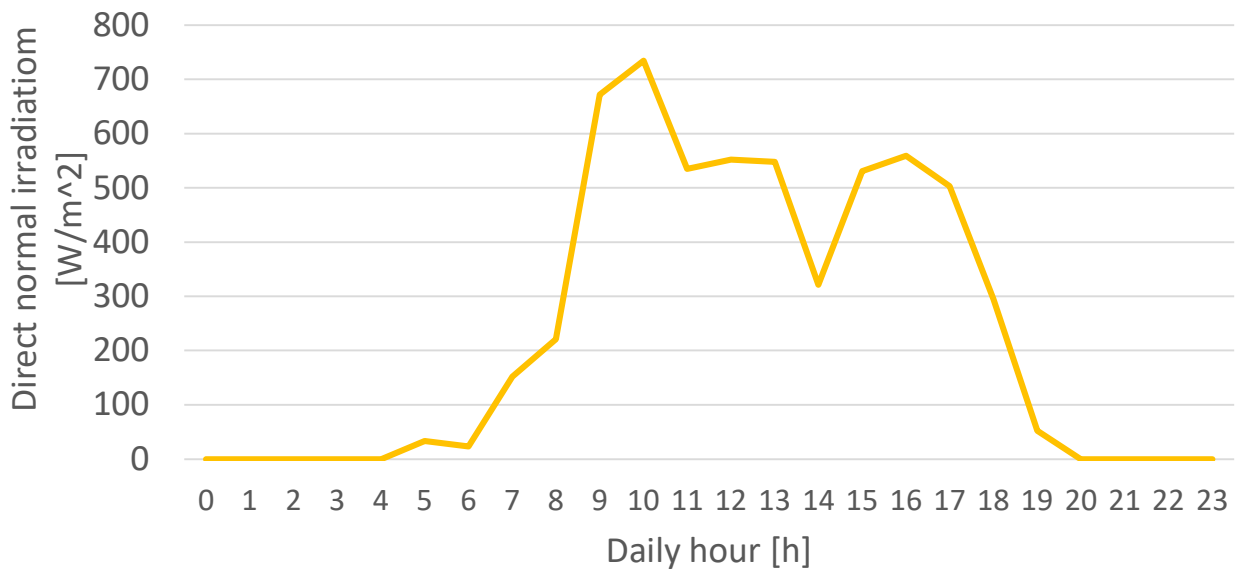


Figure 16 - The DNI trend during June 9, 2015

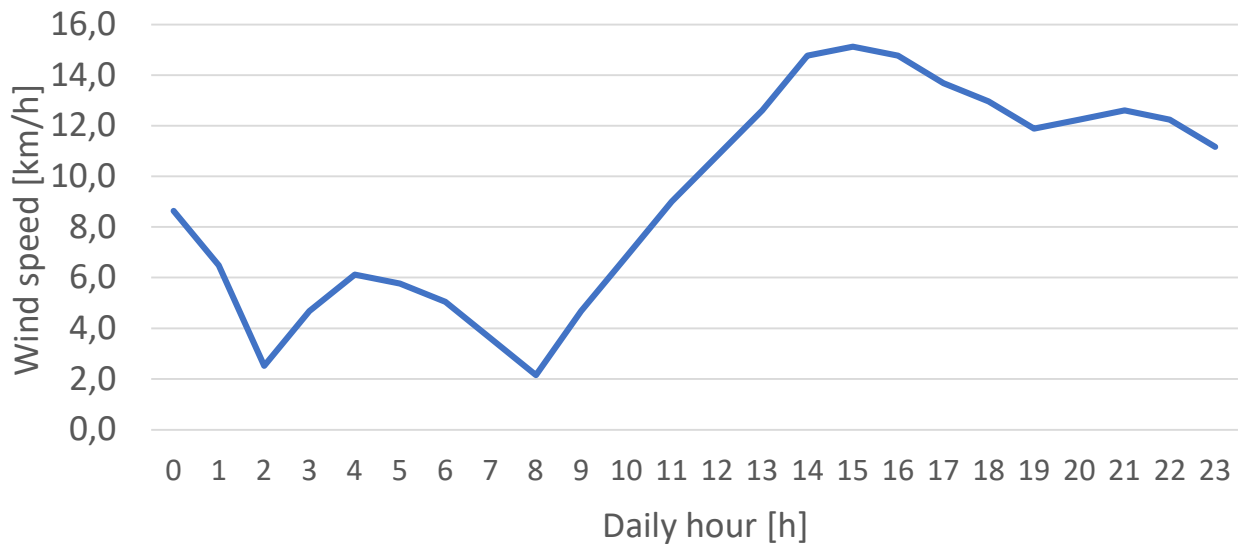


Figure 18 - The wind speed trend during June 9, 2015

It possible to see in the figures the presence of an irradiation drop, more evident around 14:00, due to the intensification of the cloud cover, persistent during the afternoon. Reversely, the temperature shows the typical oscillation of cloudy days in summer Mediterranean climates. These 30-60% DNI variations stress the pumping system, which needs to continuously regulate the flow rate to assure a stable 550°C outlet temperature. Hence, these natural conditions are the ideal framework to test the reliability of the plant to satisfy a base-load electricity demand

7.2 The regulated pump performance

The set of mass flow rate crossing the solar block and provided by FATA is shown in the Figure 19, and it is possible to see that its trend sticks to the DNI one, Figure 16. Instead, during the night the value of mass flow rate is not zero. The reason is to be found in freezing prevention, because whenever the salt solidifies, the risk of pipe cracks arises and additional operations to unfreeze the circuit become necessary.

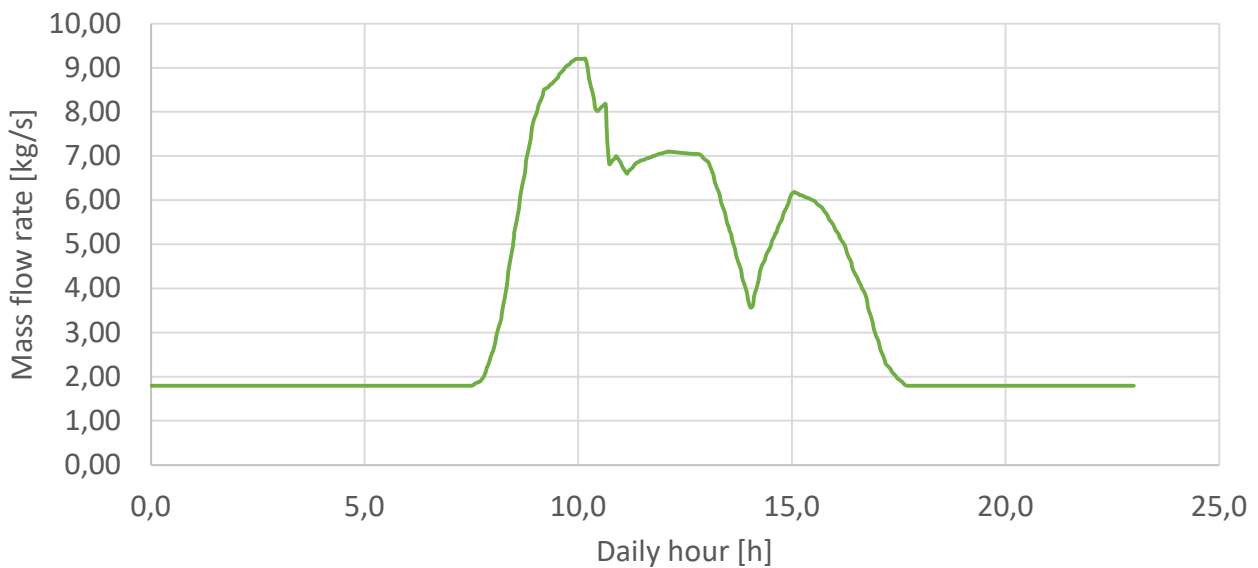


Figure 19 - The mass flow rate chart provided by FATA E.P.C.

In the Figure 20, a screenshot of the setup developed on Modelica is shown to point out the framework in which this mass flow rate set is used. The CT, located on the left, provides the salts that are heated up in the receiver by the solar field sub-model, and then they reach the HT located on the right. The HTF handling is performed by the pump, driven by the set of mass flow rate shown in the Figure 19. As inputs, the three sets of meteorological data available are used to the best stick to the real conditions.

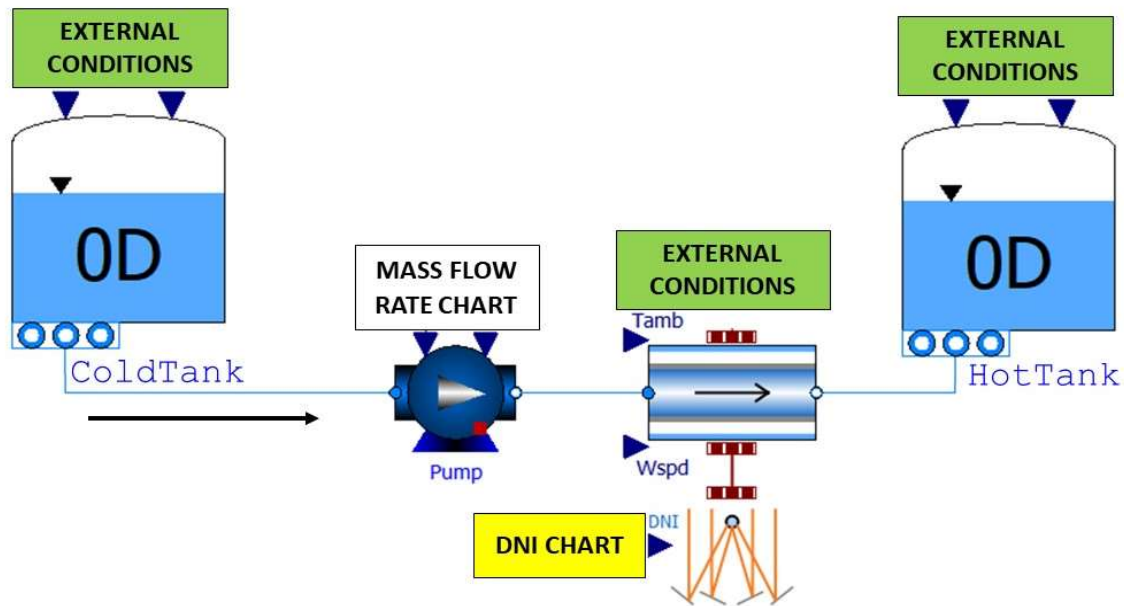


Figure 20 - Screenshot of the sub-models carrying the simulations out

The result of the simulation of this model provides the inlet and outlet temperature of the solar block, shown in the Figure 21. During daylight hours, the outlet temperature (direct towards the HT) is slightly higher than its reference (545°C) because in this model the presence of a delivery pipe (where distributed losses can arise) is neglected, hence the fluid at the inlet of the solar field results to be hotter (around 290°C) than it should. Anyway, the values settle below phase-change limit for all day.

In parallel, during the night the solar salt is kept in safe condition: the exposition to the night sky produces a non-negligible loss of temperature, hence the HTF cannot stay in the receiver but it needs to be extracted by the cold tank, recirculated and sent to the backup burner to be reintroduced to the CT. In this simulation, the presence of the backup burner is not considered, but the mass flow rate is high enough to prevent the salt solidification.

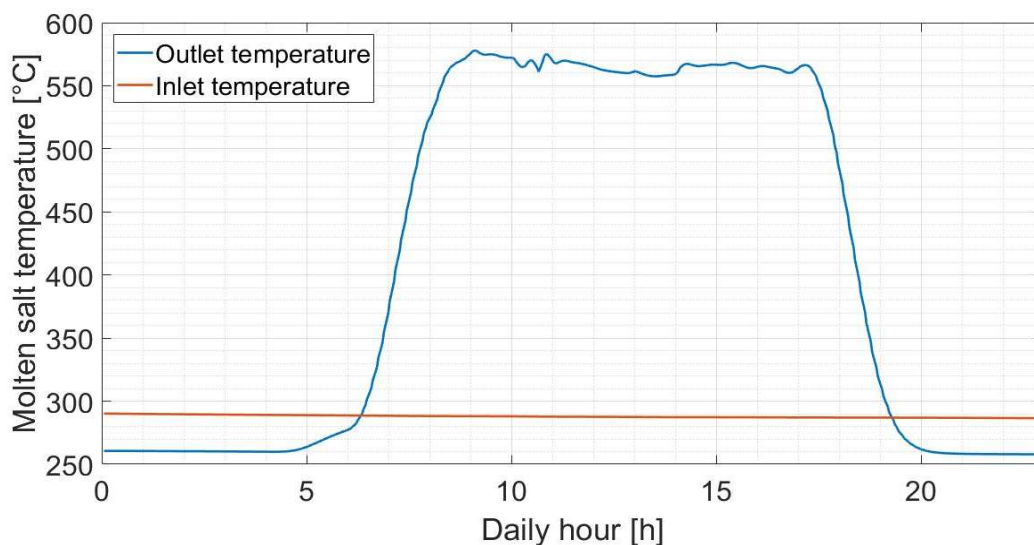


Figure 21 - The temperature evolution at the outlet solar block

Exploiting the partial plant configuration shown in the Figure 20, a simulation has been carried out in time interval between 7:00 and 18:00 with the same initial (545°C in the HT, 290°C in the CT, both filled at 40%) and boundary conditions, namely in the period when the solar field is expected to supply energy. In the Figure 22, the temperature measured at the inlet of the HT and the bulk value are reports. It is interesting to highlight a moderate stability of the first, despite a strong variability of solar energy (see Figure 16). The morning and evening ramps last around 2 hours and they are the periods in which the backup burner should come into operation as a complement to assure an additional gain for the hot tank. Then, it is possible to observe the dynamic response of the hot tank bulk fluid to the mixing with other salt. The temperature decreases before 8:00, as expectable, but then increases and it does it quickly when the temperature difference is higher, between 9:00 and 11:00.

This simulation can show that this regulation of the pump can make the solar field produce hot fluid without any needed to run the backup system, even though the solar irradiance is subject to 60% oscillations like at 14:00.

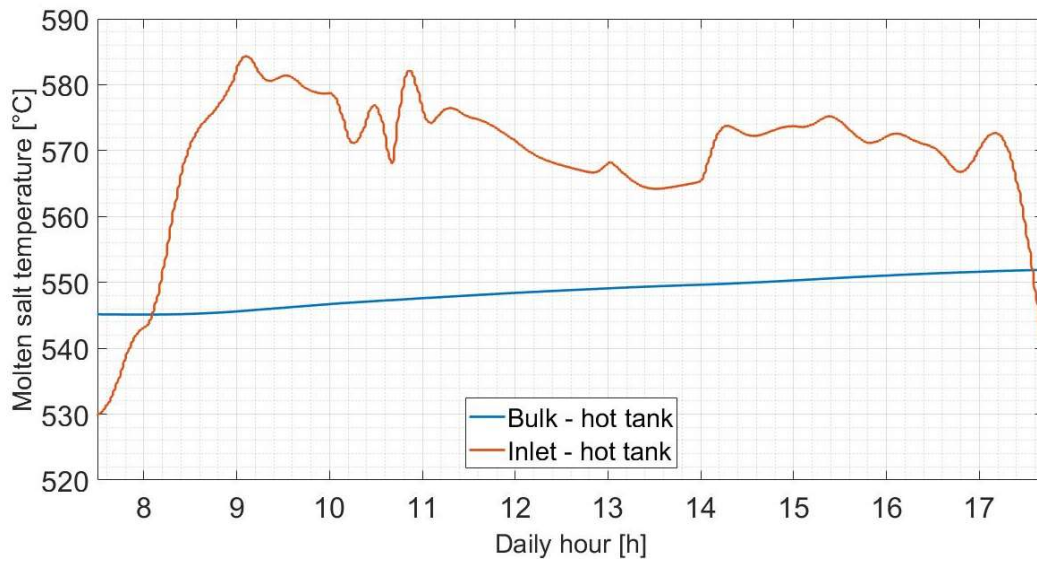


Figure 22 - The second simulation temperature evolutions

Finally, focusing on the fluid level stored in the tanks, it is possible to observe a net displacement of the fluid from the CT to the HT handled by the pump. What catches the eye in the Figure 23, is that the derivatives of the curves (which are symmetrical, as well) perfectly match the behavior of the mass flow rate pumped into the hot tank. This aspect was predictable and satisfactory, thus it is possible to conclude that the model about the tanks works in the correct way and it is reliable for several uses.

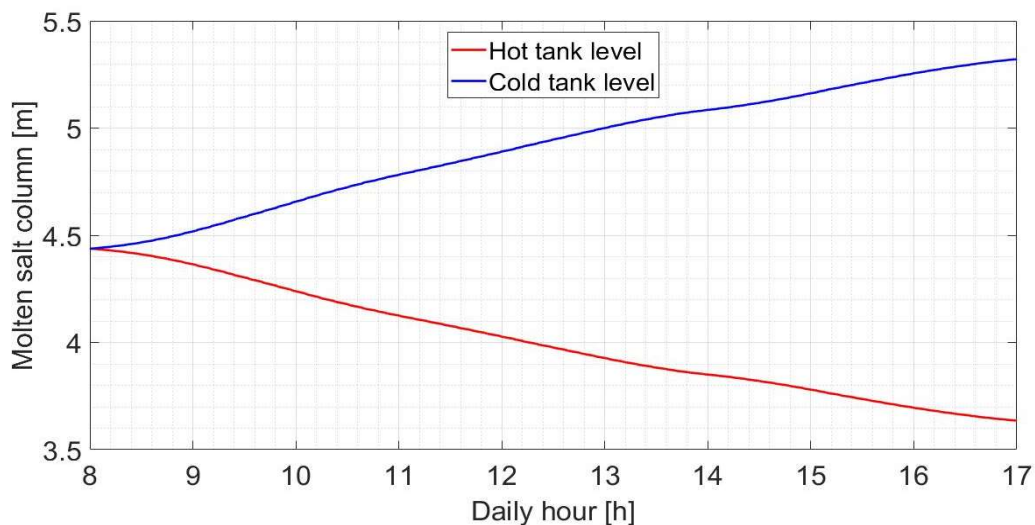


Figure 23 - The evolution of the fluid levels in the two tanks

As a conclusion, we can assert that the tank model is reliable and the dynamic behaviors of the variables considered are plausible. In the following paragraph, more detailed simulations of the entire plant are proposed to show an overall view.

7.3 The complete system simulation

The models developed in this thesis are expected to be inserted into a system-level simulation. As mentioned above, the branch of the plant dedicated to the solar block is connected to a pump which also feeds the backup, triggered on-demand, while the other line is completely dedicated to the power block. The backup activation is operated by a proper control system, that out of the scope of this thesis.

In this thesis, the complete plant (devoid of the control system) has been assembled and then simulated in two configurations. The Figure 24 reports the final structure and the conditions at which the plant is supposed to work.

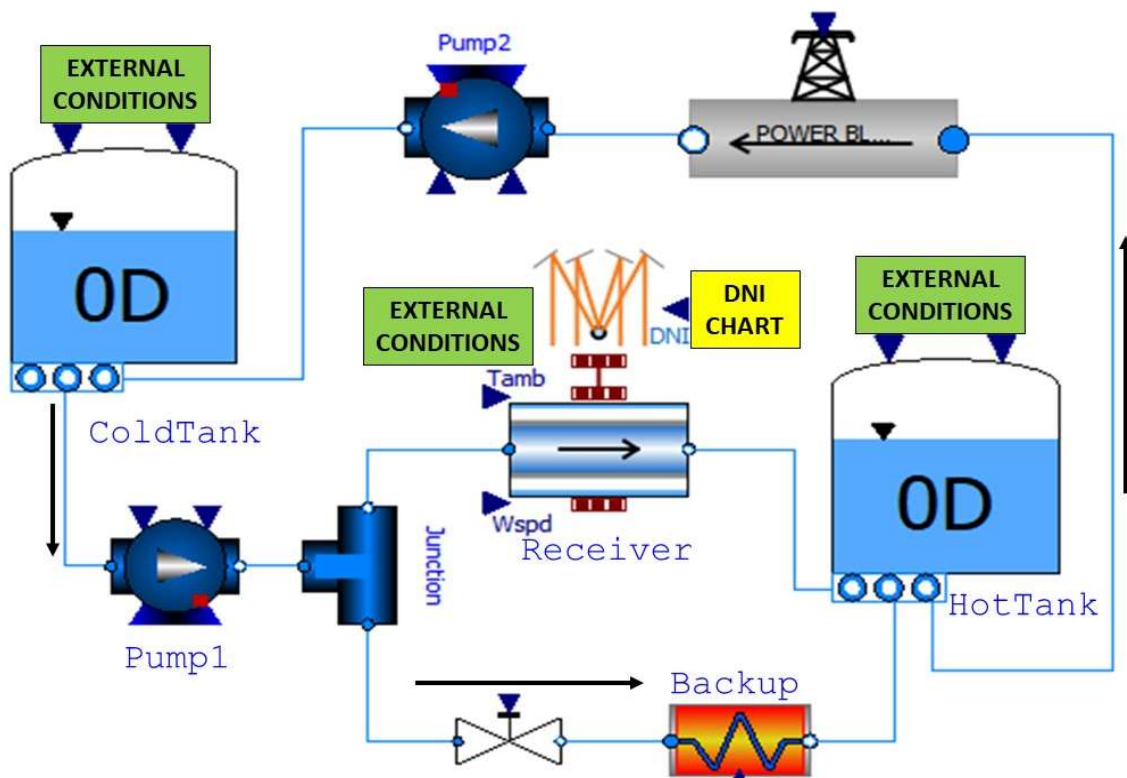


Figure 24 - A screenshot of the sub-models composing the complete plant

In the first configuration, the mass flow rate set provided by FATA and presented in Figure 19 is imposed for the pump 1 in the branch of the solar field; therefore, the valve upstream of the backup burner (that is kept off) remains closed, to let all the fluid reach the solar field. This solution allows to obtain an outlet temperature consistent with plausible values. The power block branch, instead, is supposed to work in a stationary condition, handled by the pump 2 delivering a 3.8 MW_{th} load to the heat exchanger.

For what concerns initial conditions, they consist of a 40% CT and 80% HT filling percentage, while for the boundary conditions the data sets about weather conditions (DNI in Figure 16, wind speed in Figure 18 and ambient temperature in Figure 17) dating June 9, 2015 have been adopted to stick to real conditions. The simulation has been performed in the time period between 00:00 and 24:00.

As result, the temperature evolution during the day is very similar to the profile got in the one-branch configuration, simulated above (Figure 21); this was expectable, because the conditions in which both the pump and the solar block are required to are the same and the only small difference consists of an undetectable oscillation (less than 2°C) of the CT bulk temperature.

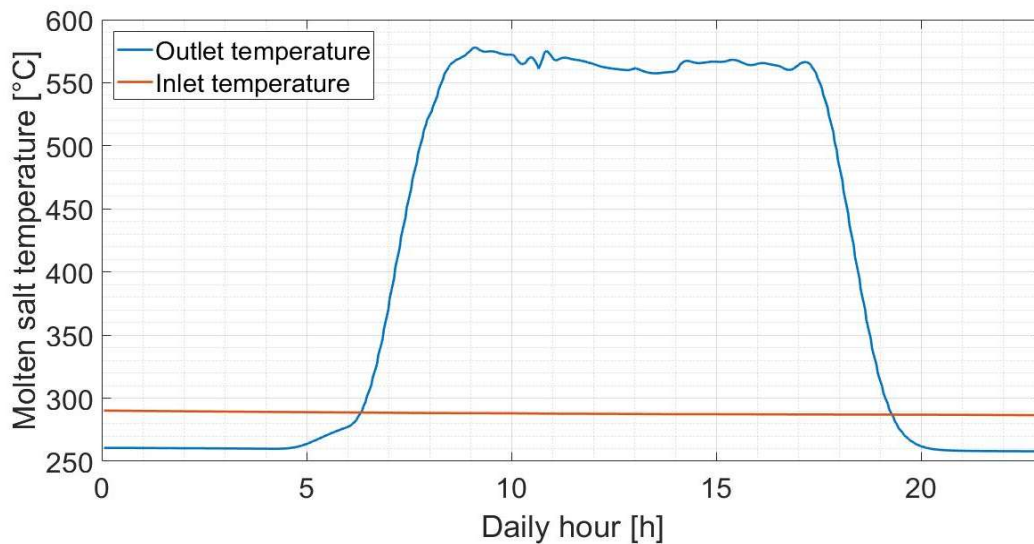


Figure 26 - The outlet temperature of the solar block for the complete plant

But in this case, since the simulation is performed along all the 24 hours and no control system can intervene to deviate and heat the cold fluid during the night, a 265°C salt flow coming from the solar field is directly sent to the HT. The introduction of a relatively cold fluid into this tank involves a temperature drop at night, visible in the Figure 256.

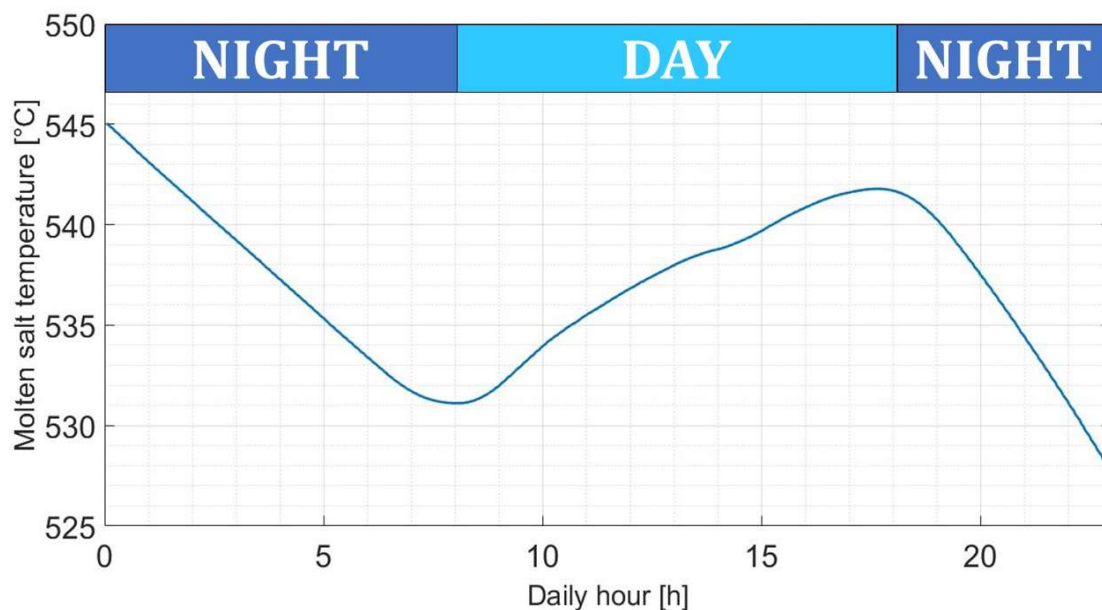


Figure 25 - The HT temperature evolution

7.4 The morning startup simulation

The last simulation performed in this thesis regards the startup condition of the solar field and the shutdown of the backup burner. The plant setup is the one reported in the Figure 24. The initial conditions consist of a 40% CT and 80% HT filling percentage, while for the boundary conditions the data sets about weather conditions (DNI in Figure 16, wind speed in Figure 18 and ambient temperature in Figure 17) dating June 9, 2015 have been adopted to stick to real conditions. The simulation has been performed in the time period between 00:00 and 8:30.

At night, the backup is supposed to work at nominal condition, heating nominal mass flow rate (around 4 kg/s) coming from the CT up to 540°C. In parallel, the flow rate in the receiver is maintained at a minimum condition (about 2 kg/s), to prevent freezing. At 7:40 backup burner is turned off and 5

minutes later the valve is closed (the opening fraction is forced to switch from 100% to 2% in few minutes, Figure 28), to simulate the occurrence of a shutdown.

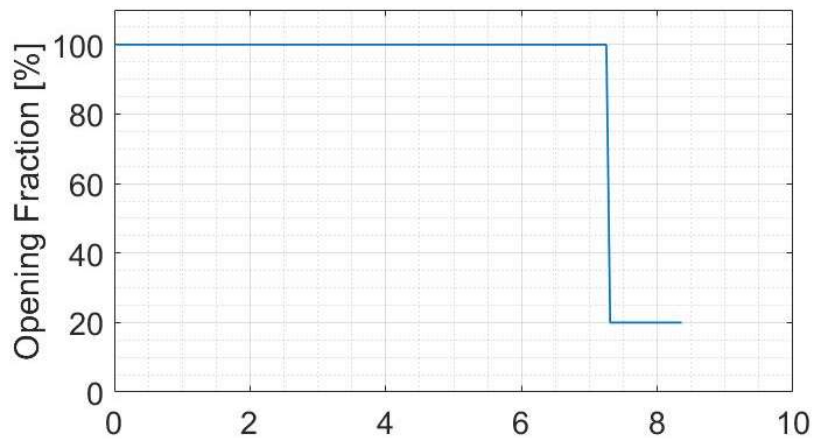


Figure 28 - The opening fraction of the valve

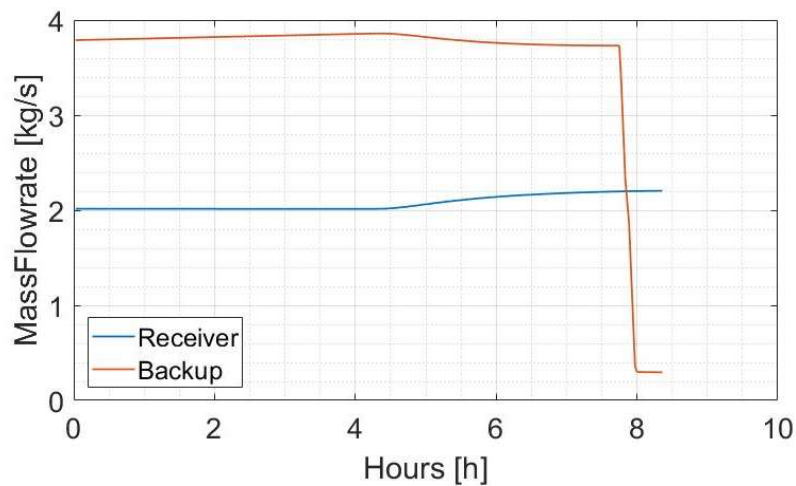


Figure 27 - The mass flow rate regulation

In the Figure 27, the effect on the mass flow rate is reported. The inflection point visible at 4:15 is due to the mass flow rate increasing in the pump, while between 7:45 and 8:00 the flow in backup burner is quickly reduced (a minimum value is anyway supposed to prevent freezing).

Finally, the temperature in the backup burner and in the receiver are shown in the Figure 29. Since the boiler is turned off 5 minutes before, a temperature drop occurs before the shutdown. The anti-freezing task of the minimum flow rate in the solar field is correctly performed.

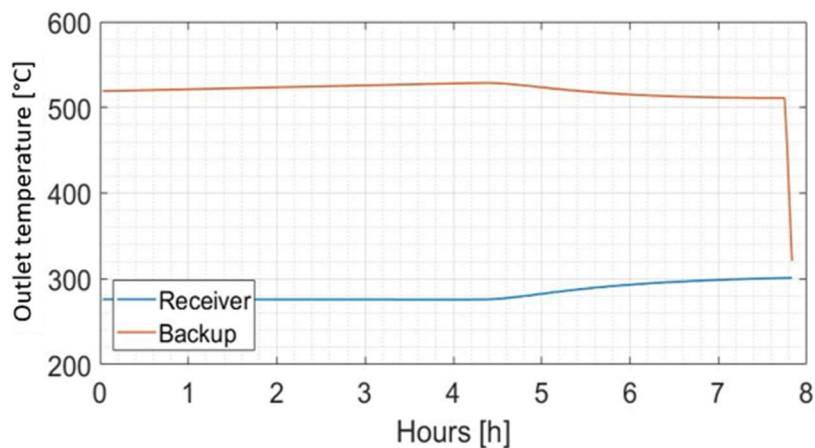


Figure 29 - The night and morning temperatures in the backup burner and in the solar field

8. Conclusions

All the models developed in this thesis provide satisfactory results, coherent to the reference values available. However, such results obtained by the system level simulations are consistent to the ones prevented and measured by FATA E.P.C.

The plant is capable of working in both stationary and simple dynamic conditions, despite the absence of a control system. Each component can show plausible values as the requested output, in terms of energy performance and thermodynamic states.

9. Perspectives

CSP plants by their very nature are subject to strong oscillations. The main limit of this thesis has been the absence of a control system, capable of handling the mass flow rate in the solar block. Although the development of such a device is not simple, due to the presence of long lines which require a proper time to accomplish the signal, it would be fundamental to perform more detailed simulation.

The tanks are the most complex devices hence a series of assumptions have been made. The relating model can be enhanced by treating these issues with different and more detailed approaches. For instance, the concrete basement has been considered as a simple resistance (supposing a conservative configuration), but a cooling system (working by natural convection) is present in the plant at Partanna.

At the same way, an enlarged system-level model could be developed considering all the possible cases in which the combination of the backup burner and the solar block are required to work. For example, the recirculation of the molten salt to prevent cold tank freezing can be simulated. Anyway, in order to deepen the analysis, a control system is mandatory to put in connection all the cases.

Finally, complete weather and mass flow rate data were provided only for one day, June 9, 2015. It would be interesting to simulate other days in other seasons, for instance during the winter.

10. Bibliography

- [1] F. Meneguzzo, R. Ciriminna, L. Albanese and M. Pagliaro, "The great solar boom: a global perspective into the far reaching impact of an unexpected energy revolution," *Energy Science & Engineering*, 2015.
- [2] C. Camy, C. Mansilla, P. Da Costa, G. Mathonniere, T. Duquesnoy and A. Baschwitz, "Nuclear and intermittent renewables: Two compatible supply options? The case of the French power mix," *Elsevier, Energy Policy*, vol. Volume 95, pp. 135-146, 2016.
- [3] International Energy Agency, "Data and statistics," [Online]. Available: <https://tinyurl.com/y223zy34>. [Accessed 15 March 2021].
- [4] J. Littlefield, J. Marriott, G. Shivley and T. Skone, "Synthesis of recent ground-level methane emission measurements from the U.S. natural gas supply chain," *Journal of Cleaner Production*, vol. 148, pp. 118-126, 2017.
- [5] S. Ashok, "Solar Energy," Britannica, [Online]. Available: <https://www.britannica.com/science/solar-energy>. [Accessed 15 March 2021].
- [6] P. Wolfram, T. Wiedmann and M. Diesendorf, "Carbon footprint scenarios for renewable electricity in Australia," *Elsevier, Journal of Cleaner Production*, vol. 124, pp. 236-245, 2016.
- [7] State of California, May 2019. [Online]. Available: <https://tinyurl.com/4z75s688>. [Accessed 15 March 2021].
- [8] State of California, May 2019. [Online]. Available: <https://tinyurl.com/5jf4ca3b>. [Accessed 15 March 2021].
- [9] European Parliament, "News," 8 October 2020. [Online]. Available: <https://www.europarl.europa.eu/news/en/headlines/priorities/climate-change/20190926STO62270/what-is-carbon-neutrality-and-how-can-it-be-achieved-by-2050>. [Accessed 15 March 2021].
- [10] Delegation of the European Union to the Republic of Moldova, "China carbon neutrality in 2060: a possible game changer for climate," 23 October 2020. [Online]. Available: https://eeas.europa.eu/delegations/moldova/87431/china-carbon-neutrality-2060-possible-game-changer-climate_en. [Accessed 15 March 2021].
- [11] United nations - Climate Change, "Carbon Neutral Government Program | Canada," [Online]. Available: <https://unfccc.int/climate-action/momentum-for-change/climate-neutral-now/carbon-neutral-government-program-canada>. [Accessed 15 March 2021].
- [12] International Energy Agency, "Concentrated solar power, technology roadmap," International Energy Agency, 2010.
- [13] C. Wang and D. Mu, "An LCA Study of an Electricity Coal Supply Chain," *Omnia Science, Journal of Industrial Engineering and Management*, vol. 7, pp. 311-335, 2014.
- [14] T. W. Africa, "Archimedes through the Looking-Glass," *Classical World*, vol. 68, pp. 305-308, 1975.

- [15] K. Butti and J. Perlin, *A Golden Thread: 2500 Years of Solar Architecture and Technology*, Cheshire Books, 1980.
- [16] Helios CSP, "Concentrated solar power had a global total installed capacity of 6,451 MW in 2019," 2 February 2020. [Online]. Available: <http://helioscsp.com/concentrated-solar-power-had-a-global-total-installed-capacity-of-6451-mw-in-2019/>. [Accessed 15 March 2021].
- [17] J. K. Kaldellis, M. Kapsali and K. A. Kavadias, "Temperature and wind speed impact on the efficiency of PV," *Elsevier - Renewable Energy*, vol. 66, pp. 612-624, 2013.
- [18] K. Mohammadi, M. Saghafifar, K. Ellingwood and K. Powell, "Hybrid concentrated solar power - desalination systems: A review," *Elsevier - Desalination*, vol. 468, 2019.
- [19] S. Ong, C. Campbell, P. Denholm, R. Margoli and G. Heath, "Land-Use Requirements for Solar Power Plants in the United States," National renewable energy laboratory, 2013.
- [20] G. P. H. Vincent K.M. Cheng, "Life-cycle energy densities and land-take requirements of various," *Elsevier - Journal of the Energy Institute*, vol. 90, pp. 201-213, 2017.
- [21] P. Heller, *The Performance of Concentrated Solar Power Systems: Analysis, Measurement and Assessment*, Woodhead Publishing, 2017.
- [22] R. Perez, P. Ineichen, E. Maxwell, R. Seals and A. Zelenka, "Dynamic models for hourly global-to-direct irradiance conversion," Denver, 1991.
- [23] P. Blanc and L. Wald, "On the effective solar zenith and azimuth angles to use with measurements of hourly irradiation," vol. 13, pp. 1-6, 2016.
- [24] Archimede solar energy, "Molten salts properties," [Online]. Available: http://www.archimedesolarenergy.it/molten_salt.htm. [Accessed 16 March 2021].
- [25] S. M. Flueckiger, Z. Yang and S. V. Garimella, "Review of Molten-Salt Thermocline Tank Modeling for Solar Thermal Energy Storage," *Heat Transfer Engineering*, 2013.
- [26] L. Cabeza, I. Martorell, L. Miró, A. Fernández and C. Barreneche, *Advances in Thermal Energy Storage Systems*, Woodhead Publishing Series in Energy, 2015.
- [27] H. Niyas and M. Palanisamy, "Comparison of Thermal Characteristics of Sensible and Latent Heat Storage Materials Encapsulated in Different Capsule Configurations," *Concentrated Solar Thermal Energy Technologies*, p. 11, 2018.
- [28] I. Rodríguez, C. Pérez-Segarra, O. Lehmkuhl and A. Oliva, "Modular object-oriented methodology for the resolution of molten salt storage for CSP plants," *Elsevier - Applied Energy*, vol. 109, p. 402-414, 2013.
- [29] M. Liu, W. Saman and F. Bruno, "Review on storage materials and thermal performance enhancement techniques for high temperature phase change thermal systems," 2012.
- [30] B. Corona, G. S. Miguel and E. Cerrajero, "Life cycle assessment of concentrated solar power and the influence of hybridising with natural gas," *LCA for energy systems and for food product*, vol. 19, pp. 1264-1275, 2014.

- [31] O. Behar, A. Khellaf, K. Mohammedi and S. Ait-Kaci, "A review of integrated solar combined cycle system (ISCCS) with a parabolic trough technology," *Elsevier - Renewable and Sustainable Energy Reviews*, vol. 39, pp. 223-250, 2014.
- [32] Modelica Association, "Modelica Language Documents," [Online]. Available: <https://www.modelica.org/documents>. [Accessed 16 March 2021].
- [33] F. Zaversky, J. Garcia-Barberena, M. Sánchez and D. Astrain, "Transient molten salt two-tank thermal storage modeling for CSP performance simulations," *Elsevier - Solar Energy*, vol. 93, pp. 294-311, 2013.
- [34] F. Kreith, R. Manglik and B. M.S., Principles of Heat Transfer, Stamford, USA: Cengage Learning, 2011.
- [35] International Energy Agency, "Concentrated solar power," [Online]. Available: <https://www.iea.org/reports/concentrating-solar-power-csp#tracking-progress>. [Accessed 15 March 2021].
- [36] Global Solar Atlas, [Online]. Available: <https://globalsolaratlas.info/map>. [Accessed 15 March 2021].
- [37] Concentrating systems, [Online]. Available: <https://www.concentrating.cz/technology>. [Accessed 16 March 2021].
- [38] Google, "Google Map," [Online]. [Accessed 16 March 2021].
- [39] Helios CSP, "Concentrated Solar Power in U.S.," [Online]. Available: <http://helioscsp.com/concentrated-solar-power-csp-in-u-s/>. [Accessed 16 March 2021].
- [40] China solar thermal alliance, "Two solar tower plants of Shouhang goes well," [Online]. Available: <http://en.cnste.org/html/csp/2018/0918/390.html>. [Accessed 17 March 2021].
- [41] N. Abed and I. Afgan, "An extensive review of various technologies for enhancing the thermal and optical performances of parabolic trough collectors," *International journal of energy research*, pp. 5117 - 5165, 2020.
- [42] Helios CSP, "Concentrated Solar Power (CSP) in the U.S.," [Online]. Available: <https://helioscsp.com/concentrated-solar-power-csp-in-u-s/>. [Accessed 17 March 2021].